Marine and terrestrial productivity in the Mediterranean basin: are (anti)cyclonic gyres tele-connected?

Giamalaki Aikaterini

February,2012

Course Title:	Geo-information Science and Earth Observation for Environmental Modelling and Management
Level:	Master of Science (MSc)
Course Duration:	September 2010 – March 2012
Consortium Partners:	Lund University (Sweden) International Institute for Geo-information Science and Earth Observation (ITC), University of Twente (The Netherlands)

Marine and terrestrial productivity in the Mediterranean basin: are (anti)cyclonic gyres tele-connected?

by

Giamalaki Aikaterini

Thesis submittedtothe International Institute for Geo-information Science and Earth Observation, University of Twente in partial fulfilment of the requirements for the degree of Master of Science in Geo-information Science and Earth Observation forEnvironmental Modelling and Management

Thesis Assessment Board

First Examiner (Chair)Prof. Dr. A.K. Skidmore
Second Examiner (External Examiner) Dr. Z. Vekerdy
First Supervisor V. Venus
Second Supervisor Dr. Ir. C.A.M.J. de Bie

UNIVERSITY OF TWENTE.
ITC
FACULTY OF GEO-INFORMATION SCIENCE AND EARTH OBSERVATION

Disclaimer

This document describes work undertaken as part of a programme of study at the International Institute for Geo-informationScience and Earth Observation, University of Twente. All views and opinions expressed therein remain the sole responsibility of the author, and do not necessarily represent those of the institute.

…Να ζούσα και πάλι
στη θάλασσα εκεί τη ρηχή και την ήμερη,
στη θάλασσα εκεί τη πλατιά, τη μεγάλη.

Κ. Παλαμάς

…I wish I would live again
there, by the shallow and calm sea,
there, by the great and wide sea.

K. Palamas

Abstract

This study provides new evidence that the impact of gyral formations in Eastern Mediterranean Sea are not only felt locally but also influence ecosystems elsewhere, even if far apart. Life on earth relies on Primary Production and Chlorophyll a (Chla) and Normalized Difference Vegetation Index (NDVI) are proved to be its reliable indexes. Mesoscale (anti)cyclonic gyres are significant formations of the marine circulation and their pronounced presence in Mediterranen basin provokes the interest for further investigation. Despite that local influences of the Sea Surface Temperature (SST) of gyres on Chla are widely known, research about its effects in remote regions is absent. On the other hand, teleconnections between SST, Rainfall and NDVI have previously concerned the scientific community. Thus, the purpose of this research is to identify possible linkages between SST in the gyral areas and both marine and terrestrial productivity indexes. A statistical approach, applied on the online platform of IRI/LDEO data library, was used in order to let the system reveal those connections on its own. The decade 1997-2007 with monthly temporal resolution was the optimum study period due to sufficient time series availability. Pearson's Product Moment Correlations and empirical analyses illustrated significant relations between SST Anomalies of the Mersa Matruh and Samothraki Anticyclones with Chla, Rainfall and NDVI Anomalies in remote Mediterranean regions. Among all the gyres formed in the basin Mersa Matruh Anticyclone, located in Central Levantine basin, appeared to have the greatest impact during April, May and October, while Samothraki gyre developing in Northern Aegean, during September. The analysis included the identification of possible causalities of the teleconnections, based on wind and sea surface currents monthly datasets. The experiments performed here are a first step toward more complex teleconnection patterns, the further investigation of which could give a better picture of the productivity variability in the future.

Keywords: Teleconnection patterns, Primary Productivity, Chlorophyll a, NDVI, Mediterranean Sea.

Acknowledgements

My gratitude goes to European Commission and Erasmus Mundus Consortium (Lund University, Sweden and ITC, The Netherlands) for grating me a place on the GEM course. This course has expanded my horizons further more than just academic knowledge. It has been a truly rewarding, despite the difficulties, experience.

My profound gratitude goes to my first supervisor Valentijn Venus, MSc for his invaluable guidance and insightful opinions and to my second supervisor Dr. Kees de Bie for his invaluable suggestions and advises. My sincere appreciation goes to Prof. Dr. Andrew Skidmore, chairman of my examination board, for his invaluable advises and beneficial recommendations during previous presentations.

Special thanks and appreciation go to Michael Bell and Dr. Benno Blumenthal from Columbia University, New York for their patience, guidance and sharing their knowledge with me. My special thanks go also to Vasilis Valavanis and Dr. Stella Psarra from Hellenic Centre for Marine Research (H.C.M.R) and to Dr. Isidora Katara from the Portuguese National Marine Fisheries and Aquaculture Research Institute and the National Institute of Biological Resources (INRB/ IPIMAR) for their valuable advises, recommendations and support.

My special thanks and love to my classmates GEM-2010 for their continuous support, cooperation and their lovely friendship. You made me smile and kept me standing in difficult times. A special mention to Shaoqing Lu for his precious help, with his amazing programming skills. Thanks to all my friends for their encouragement and incredible “remote” support.

Finally, my deepest thanks go to my parents, Michael and Natasa, and my sister Maria, for their love, patience and continuous support. I would not have achieved anything without you.

Thank you!
Ευχαριστώ!
Katerina

Table of Contents

List of figures

List of tables

Acronyms

AW	Atlantic Water
BSW	Black Sea Water
Chla(A)	Chlorophyll a (Anomaly)
EA	Eastern Atlantic
HCMR	Hellenic Centre for Marine Reseach
MO	Mediterranean Oscillation
NAO	North Atlantic Oscillation
NDVI(A)	Normalized Difference Vegetation Index (Anomaly)
RA	Rainfall Anomaly
SST(A)	Sea Surface Temperature (Anomaly)

1. Introduction

1.1. Background and Significance

The importance of the variability of the Oceans becomes clear when studying their effect on the global climate. The sea surface plays crucial role on the interactions between Oceanic, Atmospheric and Terrestrial environment. Thus, it is of high interest the studying of linkages between those different, but yet interconnected parts in regional as well as remote spatial scales.

Two or more, neighbouring or in greater distances, geographical areas can present significant positive or negative relation between two or more variables, which is referred as a "teleconnection pattern" (Hatzaki et al., 2005). It can be presented between the marine, atmospheric and terrestrial environment. Special features formed in the marine environment, such as (anti)cyclonic gyres, can present both local as well as distant impacts.

Cyclonic and anti-cyclonic gyres (Appendix I, Fig.1) determine the general circulation and the water mass patterns in the Ocean. Those formations have various reasons of creation (e.g. wind, topography or tidal mixing) and different chemical and biological properties than the surrounding water masses (Belkin et al., 2009). The anticlockwise movement of the cyclonic gyres make them act like nutrient pumps by bringing the cold bottom water closer to the surface, which increase the nutrient concentrations and the primary productivity levels within their boundaries (Legendre et al., 1970; Siokou-Frangou et al., 2010). On the other hand, anti-cyclonic gyres present lower productivities inside their cores (Biggs, 1992) and higher productivity and nutrient concentration levels in their boundary areas (Raj et al., 2010), because of their clockwise movement that makes them function as warm water traps and transfer warm, nutrient-poor, surface water to the lower water layers. Since those formations have influence on the primary productivity, it is reasonable and proved to affect higher trophic levels, like elephant seals or pilot whales (Bost et al., 2009; Dragon et al., 2010; Hátún et al., 2009). Further from their local effects, due to discrimination of their water masses from the surrounding waters, it is expected they will present teleconnectivity with regions elsewhere.

Introduction

A marine teleconnection example is described in the publication of Cartes et al. (2011)where a change in the physical properties (temperature and salinity) of the Levantine Intermediate Water (E. Mediterranean) formed in the Rhodes Cyclonic area, due to climate changes and the creation of Nile dam in 1965, caused the extinction of a shrimp (*Aristaeomorpha foliacea*) population in the Balearic basin, with a time lag of approximately 3-5 years. Despite the fact that Chlorophyll a (Chla) is a basic parameter indicating the Primary Productivity in the sea water, research about the effects of (anti)cyclonic gyres on Chla, in remote regions, is absent. On the other hand, teleconnections between SST, rainfall and vegetation indexes have previously concerned the scientific community.

Warm SST increases the heat fluxes to the atmosphere and results increase of the precipitation events as well as their intensity, and on the contrary colder SST causes decrease of the rainfall totals (Lebeaupin et al., 2006). Mediterranean Sea presents surplus of evaporation, reaching its maximum over November (Sanchez-Gomez et al., 2011) and the eastern basin is presented to be directly related to the atmospheric conditions of the wider Mediterranean area (L. Z. X. Li, 2006). Statistical analyses have proved the teleconnection patterns between SST and rainfall changes (Lolis et al., 2004; Zhou, 2011), which usually present different time lags depending on the conditions of the area of interest (Kirono et al., 2010).

Specifically, warm SST events, especially of the eastern basin, enhance the moisture convergence and following affect the rainfall totals of the Sahel region (Rowell, 2003). In addition, those warm occurrences of the basin have greater impact on the African precipitation than the cold ones (Fontaine et al., 2010). As a consequence of the connections of SST with rainfall, and taking under consideration the direct and strong relation between precipitation and vegetation growth (Nicholson et al., 1990), the secondary relation of SST with the terrestrial productivity is expected.

One of the most intensively studied areas for teleconnection patterns for its vegetation is the African Sahel. The photosynthetic activity of the area is associated with warm Mediterranean SSTs (Philippon et al., 2007). Further, different marine areas seem to affect different Sahelian NDVI regions (Huber et al., 2011); for example high SSTs of the Mediterranean Sea is presented to influence positively the greenness of the central Sahel.

1.1.1. Marine and Terrestrial Productivity indexes

Marine primary productivity can be well described by Chla concentrations and it can be estimated by the use of algorithms that use Chla as their parameters (Isada et al., 2010). Chla is a significant index for the phytoplankton (Karydis, 2009), which is the base for primary productivity and have influence on the marine organisms of higher trophic levels (Boyce et al., 2010).

Terrestrial vegetation productivity can be monitored and assessed by the use of satellite derived NDVI. This indicator is directly and linearly related to vegetation cover (Garcia-Gomez et al., 2011) and has been used in previous studies for the monitoring of areas covered by different vegetation types in various case studies(Garcia-Gomez, et al., 2011; Maselli et al., 2009; Munyati et al., 2011). NDVI is declared as a useful source of information and suitable tool to estimate changes in productivity and condition of vegetation. It is considered to be one of the optimal indexes for the description of the vegetation state (Su et al., 2009).

As a consequence of all the above factors it has been decided to use Chla and NDVI as indexes for the studying of marine and terrestrial primary productivity in the selected study area.

1.1.2. Conceptual Framework

The most representative framework for this study is the hydrologic cycle, which describes the water movement in the Earth's system as well as the mechanisms causing it (Appendix I, Fig. 2). The general driving parameter in the water cycle is the solar radiation which is mainly absorbed by the oceans (Bigg et al., 2003). Energy, heat and water exchanges vary with geographical, physical and biological conditions (Bridgman et al., 2006). The principal underlying processes of this research are the ocean evaporation, the precipitation and the plant uptake. Ocean provides 85% of the water vapour in the atmosphere and specifically about the study area, the mean annual evaporation of the Mediterranean Sea is estimated at 1500 ± 190 mm yr^{-1} (Matsoukas et al., 2005). The condensed water vapour precipitates to the Earth's surface and in this case the possible lead, which is of interest, is the vegetation uptake.

A conceptual diagram is illustrated by Fig. 1, derived from the general objective of this research (section 1.3). The image presents the main components that could affect and be affected from the (anti)cyclonic formations. Additionally, is a simplistic representation of how the marine, atmospheric and terrestrial environments could interact with each other in the assumed closed system of the Mediterranean Sea.

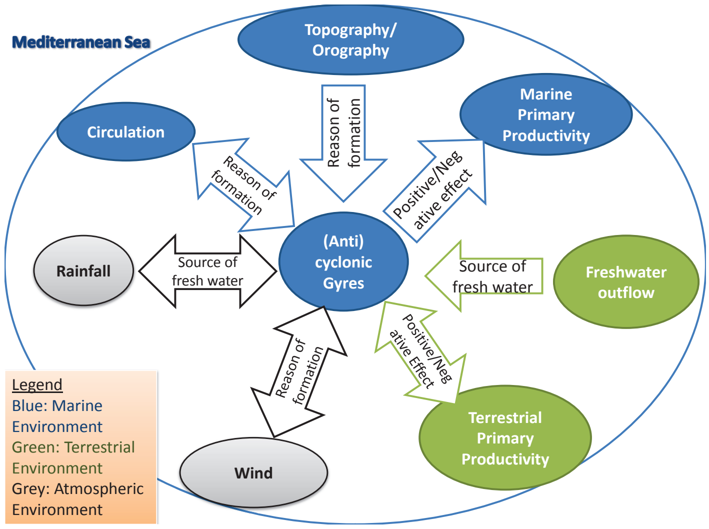

Fig.1: Conceptual Diagram.
Description of the connections between marine, atmospheric and terrestrial environment. Wind, Circulation and Topography/Orography of the area are the reasons of formation of the gyres. Rainfall and Freshwater outflows from the land are sources of freshwater in the sea. Marine and Terrestrial Primary Production can affect and be affected from (anti)cyclonic formations.

1.1.3. Terminology

Taking into consideration that our natural environment is the best model of itself, through statistical analyses it can reveal the areas of Mediterranean Sea that have positive or negative influence on the marine and terrestrial productivity levels. The name “Candidate Productivity Hotspots” was given to those important marine areas. This selection was based on the significant relations of the associated parameters; the physical and biological parameters of the regions that were investigated should be significantly and strongly correlated with each other. From those regions the “Selected Productivity Hotspots” were chosen based on the following criteria. First, in the Candidate Productivity Hotspots (anti)cyclonic gyres should be present; in case of absence of those formations the Candidate Productivity Hotspot was rejected and, second, a possible causality of the previously indicated relationships should be identified. Finally, “Productivity Hotspots” are the marine areas of the Selected

Productivity Hotspots after a second correlation set with a higher spatial resolution, in order the finalized decision to be taken (Fig.2).

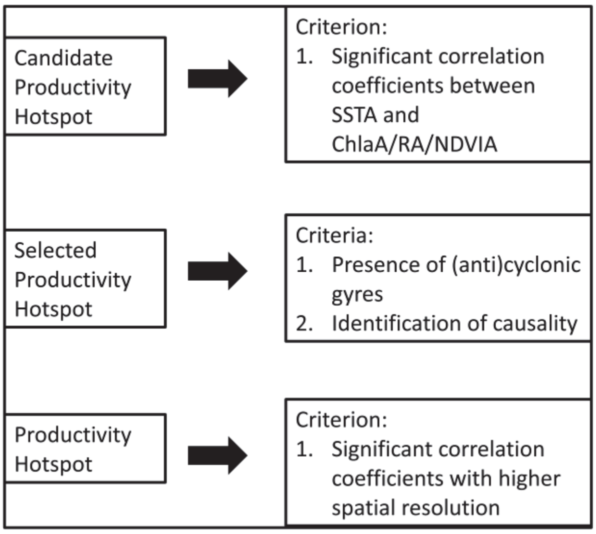

Fig.2: Illustration of the terminology used and the criteria need to be fulfilled for each term.

1.2. Research Problem

Atmospheric, terrestrial and marine environment have been widely studied either as individual or as teleconnected parts. Primary Productivity is of crucial importance for life on Earth and its indicators, such as Chla and NDVI, have widely concerned the scientific community. Similarly, oceanographers have investigated thoroughly oceanographic phenomena, such as (anti)cyclonic gyres and fronts, thus their effects on physical and biological parameters of the areas they are formed are well known. Despite those, studies describing teleconnections between (anti)cyclonic formations and marine and terrestrial productivity indexes are absent and yet the causality of those remote relations is still unexplained. This research will contribute to the better understanding of how and why, different and distant phenomena are connected with each other, but still it is a first step towards a more complex teleconnected system. Despite the fact that this is a first step of identifying the linkage between tree different parts of the environment, its complexity creates a great challenge to be investigated.

1.3. Research Objectives and Questions

The overall objective of this study is the determination of the effects of the temporal and spatial multi-year cycle of the (anti)cyclonic gyres formed in Eastern Mediterranean on marine and terrestrial primary productivity in remote areas in Mediterranean region.

Based on the above broad objective, specific objectives and their related research questions were formulated (Table 1).

Table 1: Research Objectives and Questions

	Research Objectives	**Research Questions**
1	Determination through statistical analyses of the Candidate Productivity Hotspots	Which are the Candidate Productivity Hotspots in the Eastern Mediterranean?
2	Discovery of influences of Candidate Productivity Hotspots on productivity levels of the Mediterranean Sea and its surrounding terrestrial environment (criterion regarding the strength of the relationships between examined parameters).	Do the Candidate Productivity Hotspots affect the productivity levels in the Mediterranean Sea and the surrounding terrestrial environment?
3	Examination of (anti)cyclonic gyres and identification, through specific criteria, of the Selected Productivity Hotspots (criteria: yes/no gyre and causality identification)	Which are the Selected Productivity Hotspots in the E. Mediterranean?
4	Identification of the Productivity Hotspots and studying of their influences on primary marine and terrestrial productivities.	Which are the Productivity Hotspots and how they influence the primary productivity of the area?

1.4. Hypotheses

Acknowledging the obvious effects of gyral formations coinciding with the area of their development (see Section 1.1, page 1) it has been decided that their local effects on marine productivity are excluded from this study.

Hypothesis 1:
Are there areas in the Eastern Mediterranean Sea that are teleconnected to primary productivity anomalies found elsewhere in the Mediterranean region (marine and terrestrial environments)?

H_0: Eastern Mediterranean basin's Sea Surface Temperatures are not significantly associated to Primary Productivity found elsewhere in the Mediterranean region.

$$\rho = 0$$

H_1: Eastern Mediterranean basin's Sea Surface Temperatures are significantly associated to Primary Productivity found elsewhere in the Mediterranean region.

$$\rho \neq 0$$

Where

ρ refers to the correlation coefficients of all associations tested, i.e. in order to reject the null hypothesis all the correlation coefficients of SSTA:ChlaA, SSTA:NDVIA and SSTA:RA correlations must be different from 0.

Hypothesis 2:
Do (anti)cyclonic formations systematically coincide with the areas of Eastern Mediterranean basin that have distant effects on primary productivity elsewhere in the Mediterranean region?

H_0: (Anti)cyclonic gyres do not systematically coincide with the areas of Eastern Mediterranean basin that have distant effects on primary productivity elsewhere.

$$P \leq P_{thres}$$

H_1: (Anti)cyclonic gyres systematically coincide with the areas of Eastern Mediterranean basin that have effects on Primary Productivity elsewhere.

$$P > P_{thres}$$

Where

P is the probability of presence of (anti)cyclonic formations in the areas of Eastern Mediterranean found having distant effects on Primary Productivity.

P_{thres} the threshold set at the confidence level of 95%.

1.5. Research Assumptions

This research is based on the following assumptions:

1. The linear relationship between the variables.
2. The generally excepted association between SSTA, ChlaA, RA and NDVIA holds.
3. The surfaces under study are homogeneous.
4. According to the publishers of each of the dataset used in this research, all processes for the preparation of the data (like atmospheric correction and optimum interpolation) succeeded with the expected accuracies and the resulting noise does not affect the claimed relationships.

Chapter 1

2. Materials and Methods

2.1. Study Area

Mediterranean Sea is a semi-enclosed sea, has a general cyclonic circulation (Gerin et al., 2009) and is connected to the Atlantic Ocean and Black Sea (Fig.3). It covers an approximate area of 2.5 million km^2, has an average depth of 1,500 m and is considered to be an oligotrophic sea. The climate of the area is Mediterranean Climate and is characterized by warm to hot, dry summers and mild to cool, wet winters. In this research the whole Mediterranean Sea and its surrounding terrestrial regions (10°W to 36°E and 46°N to 27°N) are considered to be the study area, but the Candidate, Selected and Productivity Hotspots were selected from the Eastern Mediterranean basin (20°E to 36°E and 41°N to 31°N).

The basin shows an excess of evaporation over freshwater inputs and a heat loss through air-sea interaction (Sanchez-Gomez, et al., 2011). It has an overall freshwater deficit, as the loss to the atmosphere by evaporation is larger than the gains by precipitation and runoff from the main rivers and input from the Black Sea.

The Mediterranean vegetation is dominated by evergreen shrubs and sclerophyllous trees adapted to the distinctive climatic regime of summer drought and cool moist winters with only sporadic frost. The most favoured time for vegetative growth is spring, when the soil is moist and the temperatures are rising, or autumn, after the first rains.

Related to the general circulation of the Sea (Appendix I, Fig. 3), the Atlantic Water (AW) variations affect the water parameters of the whole Mediterranean basin and needs at least one or two years to reach the eastern part (Beuvier et al., 2010). The AW passes through the Gibraltar and Sicilian straits to reach the Egyptian Coasts and the Levantine sub-basin and constitutes the subsurface water mass (Said et al., 2011). In winters it forms the Levantine Intermediate Water, which is flowing along the north coast of the Mediterranean Sea and becomes the outflow in the Atlantic Ocean (Menna et al., 2010). Additionally, Black Sea Water appears to contribute to dense water formation in the Aegean Sea, which is flowing into the Mediterranean through the Cretan Straits (Velaoras et al., 2010).

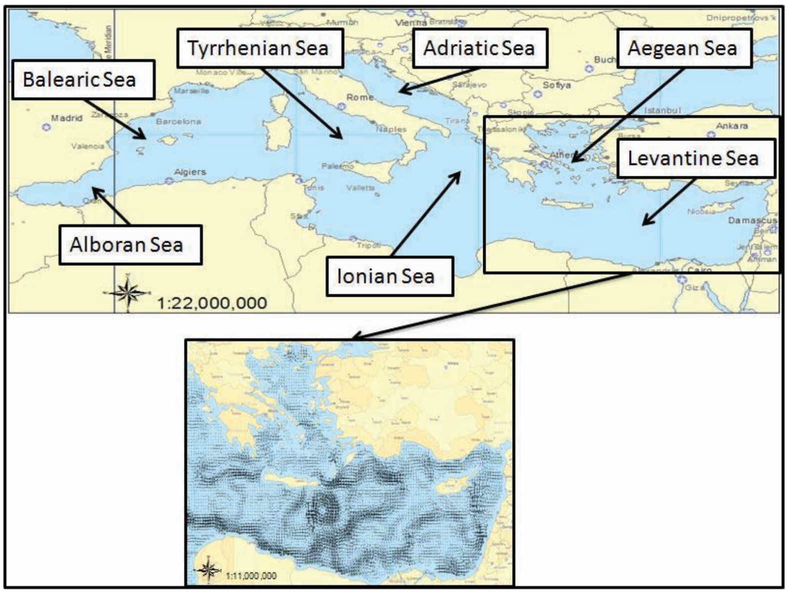

Fig.3: The Mediterranean Sea and the Eastern Mediterranean basin, including the names and locations of its sub-basins and highlighted is the general circulation pattern.

2.2. Data available

Time series can provide continuous picture of the past and present sea water circulation patterns, as well as SST and Chla concentration datasets can present in detail the general productivity of the selected region. In this research time series of Sea Surface Temperature, Chlorophyll a, Ocean Surface Currents, Rainfall, Normalized Difference Vegetation Index and Wind datasets were used. The next table (Table 2) summarizes the sources and detailed information about the obtained datasets.

Table 2: Datasets that were obtained and used in this research

Variable	***Sea Surface Temperature***	***Chloro-phyll a***	***Ocean Surface Currents (Direction & Speed)***	***Normalized Difference Vegetation Index***	***Rainfall***	***Wind (U/V)***
Source	NOAA National Oceanographic Data Center	NASA - Combined data from MERIS, MODIS and SeaWiFS	AVISO-Merged T/P, Jason-1, ERS-2, Envisat	NASA- Data by continent by AVHRR	NOAA National Climatic Data Center	NOAA/ NOMADS
Available in	IRI/LDEO Data Library	ITC Data Server	HCMR Data Library	IRI/LDEO Data Library	IRI/LDEO Data Library	IRI/LDEO Data Library
Available from	1982 - 2009	1997-2008	1992-ongoing	1981-2007	1979-2010	1870-2008
Spatial resolution	1x1 deg	0.08x0.08 deg	1/8x1/8 deg	0.07x0.07 deg	2.5x2.5 deg	2x2 deg
Temporal resolution	Monthly	Monthly	Monthly	15 Days	Monthly	Monthly
Units	°C	mgm^{-3}	cm/sec	Unitless	mm	m/s

Most of the data (SST, NDVI, Rainfall and Wind) were available on the IRI/LDEO Data Library (IRI/LDEO Climatic Data Library, 2011) and were directly used in the analysis. Chlorophyll a dataset was obtained from ITC Data Server and had to be imported to the IRI/LDEO Data Library in order to be used in the statistical analyses. Personal communication with personnel from Columbia University responsible for the Data Library made the importing of the data possible. The graphs (Fig. 4) illustrate the decadal variations of the data that were used for the correlation statistical analyses for the study period (1997-2007). Further, the sea surface currents data needed additional symbology processing in ArcMap for the production of the velocity vectors, because two different sets including speed and direction were obtained. Their source was the Hellenic Center for Marine Research (HCMR) data library and they were obtained from personal communication as well.

Regarding the Wind dataset, U and V components were processed in order to obtain the wind velocity vectors in IRI/LDEO Data Library. Despite the fact that different atmospheric pressure levels were available (from 10mb to 1000mb), the 850mb level was used since it is above the boundary layers, it is not affected from surface friction and is usually used to diagnose thermal advection that forces the precipitation systems (McGill University, 2003).

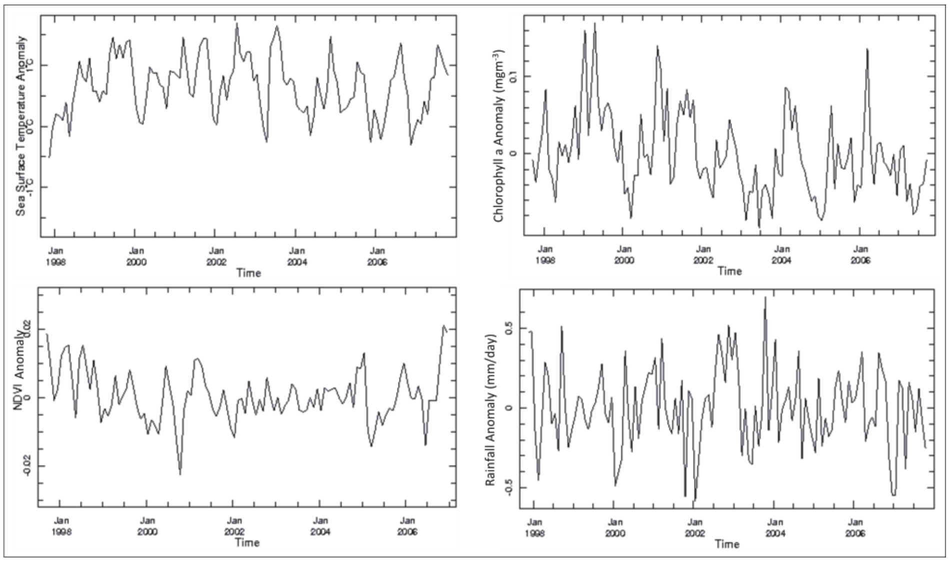

Fig.4: Graphical representation of the time series of the four variables used for the years 1997-2007.
SST, Chla, NDVI and Rainfall anomalies throughout the examined decade are illustrated.

2.3. Methods

The first part of the analysis has been held with three different time groupings of the datasets; the decadal, the seasonal and finally the monthly analysis. The decadal analysis has been rejected since its results were presented to be very general for the purpose of this study and also it was not taking under consideration the intense seasonal SST variations of the study area between cold and warm periods (Marullo et al., 1999). Seasonal analysis was decided not to be used because the monthly variability of the (anti)cyclonic formations in Eastern Mediterranean could not be depicted correctly after the seasonal averaging. Finally, the monthly analysis was selected as the most proper one that represents actual alternations of both SST and sea surface currents. All the “productivity hotspots” terms that are used, describe marine areas based on SST regions (SSTA pixels) and their selection was based on the criteria mentioned before (section 1.1.3).

Initially, Shapiro – Wilk normality tests were held in Matlab, for each pixel and each month separately (Fig. 6, part a), for all the 4 variables used in the correlation process.

All the following correlation analyses were processed in IRI/LDEO data library of Columbia University (Columbia University, 2011). The computer language used was the Ingrid PostScript-based Language(IRI/LDEO Climatic Data Library, 2011). Based on the results of the normality tests, Pearson Product Moment monthly correlations between the predictor SSTA and each one of the predictands (NDVIA, RA and ChlaA) were held throughout time (Fig. 6, part b). The spatial resolution of all variables at this step was 1x1 degree lat/lon. Each pixel of SSTA in Eastern Mediterranean (20E to 36E and 41N to 31N) was correlated with all the pixels of the whole Mediterranean area (10W to 40E, 46N to 27N) on a monthly basis for the 10 years. The resulting maps illustrated all the pixels of the predictands that presented significant correlation coefficients as well as the value in each pixel. This process was held for all the three predictands separately. An example of the process is presented in Fig. 5 and the procedure in mathematical terms is described in section 2.4.2.

Additionally, for each predictand three time lags were tested in order to reveal the highest significant correlations between them as well as the ideal time lag that should be used for each variable. First, for all the predictands, correlation coefficients were calculated without time lag. For the NDVIA two and three months time lags and for the RA one and two months time lags correlation coefficients were calculated. For the ChlaA, six and twelve months lags were chosen.

By the end of the first set of correlations, SSTA pixels were selected, taking into consideration the highest significant correlation coefficient of the best time lag, for each variable, for each month, the combination of which resulted the Candidate Productivity Hotspots (Fig. 6). The degrees of freedom used in every correlation were 8 and the confidence interval for the significant r was 0,716 at the 98% significance level (α=0.02).

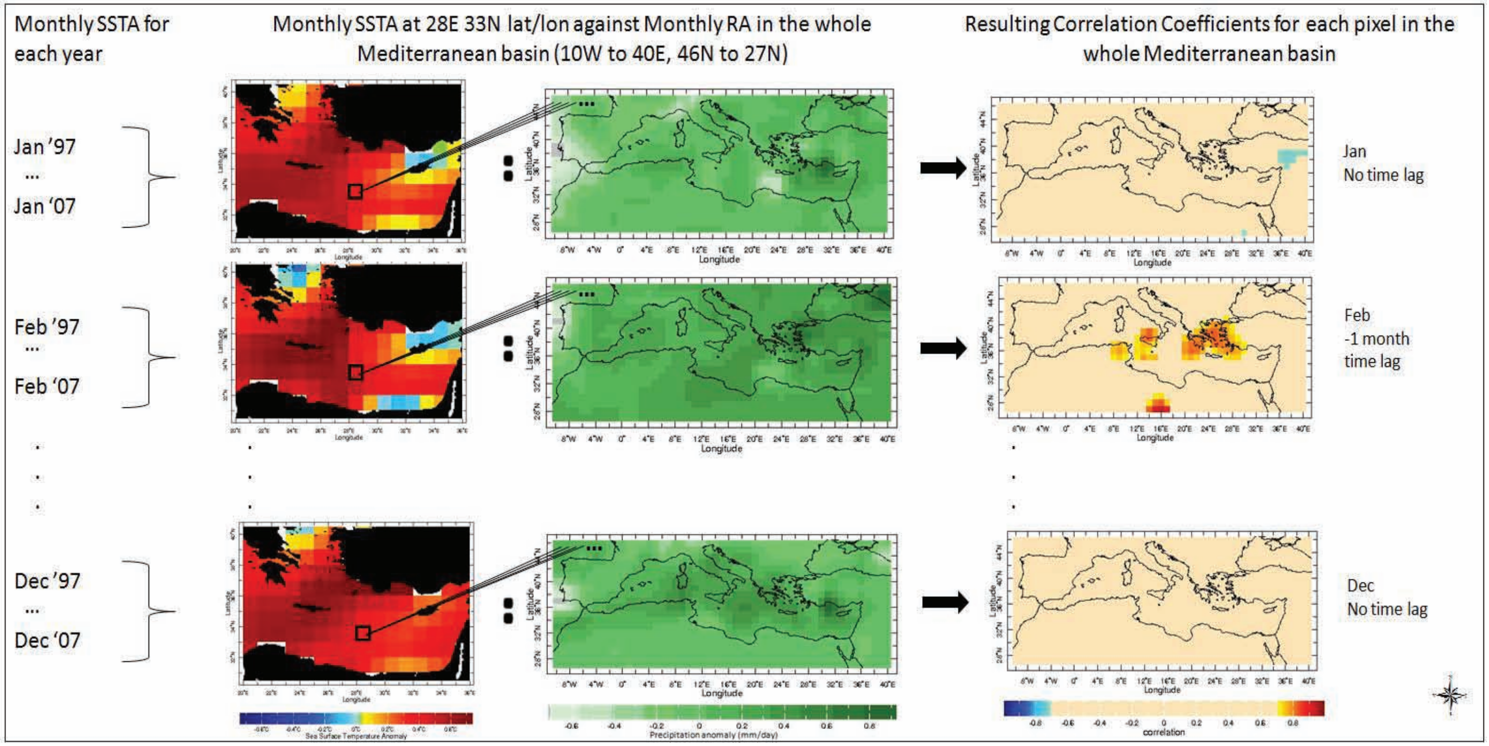

Fig.5: Example for the description of Pearson Correlation's process.
The monthly SSTA for the 10 years in the pixel 28E, 33N lat/lon is correlated with the monthly RA of the corresponding year of each pixel of the Mediterranean region (10W to 40E, 46N to 27N) and the resulting map presents the Correlation Coefficients in each pixel in the whole area. Different time lags are also presented, depending on which has showed the higher correlation coefficients. In Beige colour are the pixels that did not present significant correlation coefficients, while coloured are the significant values.

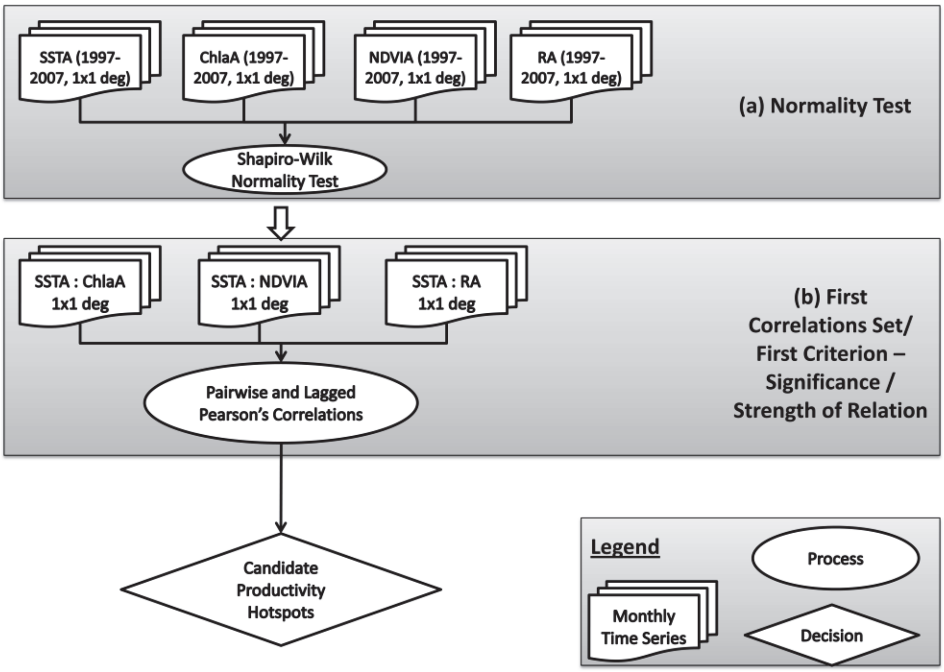

Fig.6: First part of the followed methodology.

As a continuation, the Candidate Productivity Hotspots were imported in ArcGIS 10 and overlaid with the Sea Surface Currents velocity vectors. Monthly surface currents were used, since the seasonal and decadal averaging of the velocity vectors was not representative of the Eastern Mediterranean circulation.

The pixels of the Candidate Productivity Hotspots that included (anti)cyclonic gyres formatted in the area (Fig. 7) for more than seven out of the ten years were chosen to constitute the Preselected Productivity Hotspots (Fig.9, part c). The traditional threshold for Presence/Absence analyses is usually set to 0.5 as the cut-off value (Freeman et al., 2008). The significance of this threshold was tested by calculating its confidence intervals with the use of the method proposed by Agresti and Coull (1998). The single-sided confidence interval was calculated, since the lower limit was of interest and any value higher that that should be acceptable (statistical test regarding the second hypothesis, section 1.4). At a 95% significance level the single-side confidence interval was 0.64, which indicates that the threshold set (0.5) is not statistically significant. The threshold allowed to be used from the results of this single-sided confidence interval calculation was 0.7, which shows that gyres should be present at least seven out of the ten years examined.

Following, all the correlation coefficients were transformed to positive, since the sign of the relationship is not important at this step, and the mean values of the correlation coefficients were calculated for each predictand, each pixel of the Preselected Productivity Hotspot and each month and a graphical representation of them was produced.

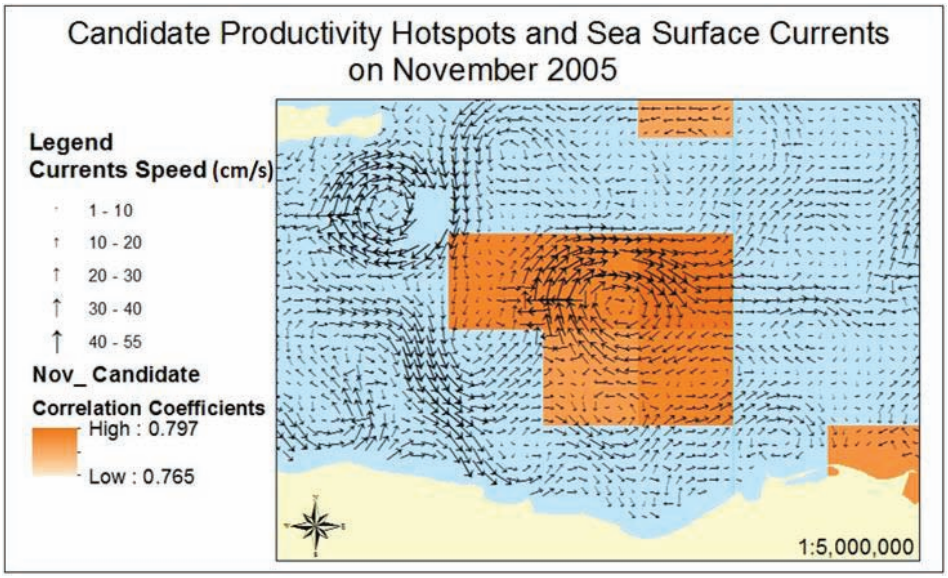

Fig.7: Example of November Candidate Productivity Hotspots and Sea Surface Currents on November 2005 in Central Levantine Basin overlaid in order to fulfil the second criterion regarding the presence or absence of the (anti)cyclonic gyres within the hotspot's area. In this example the group of two SSTA pixels that include the Mersa Matruh anticyclone will be chosen as Preselected Productivity Hotspot, while the single SSTA pixels should be rejected.

Only the Preselected Productivity Hotspots were used in the next step, in which the resulting correlation maps presenting the correlation coefficients of the pixels of each predictand (such as RA maps in Fig. 5) were overlaid with the monthly Sea Surface Currents and Winds (Fig. 8) of the study area, in order to reveal any possible direct causality of the previously observed relations (Fig. 9, part d). Once the causality of the effects was identified the remaining areas were named Selected Productivity Hotspots (Fig. 9).

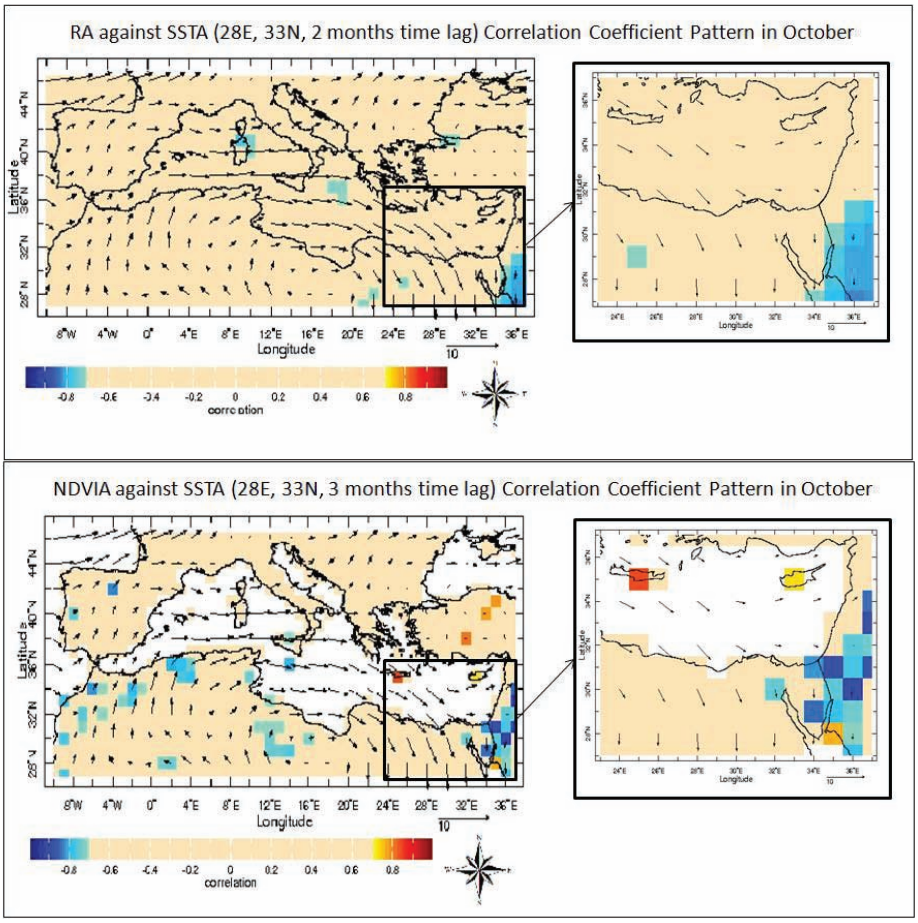

Fig.8: Example of the overlay of RA (upper map) and NDVIA (lower map) correlation coefficients of each pixel resulted from the Pearson's Correlations against SSTA (28E, 33N pixel) in October with the wind pattern at 850mb pressure level.
The beige colour represents the correlated areas that did not have significant coefficients. In the highlighted image the clearer wind pattern is shown as well as the main affected area of NDVIA and RA.

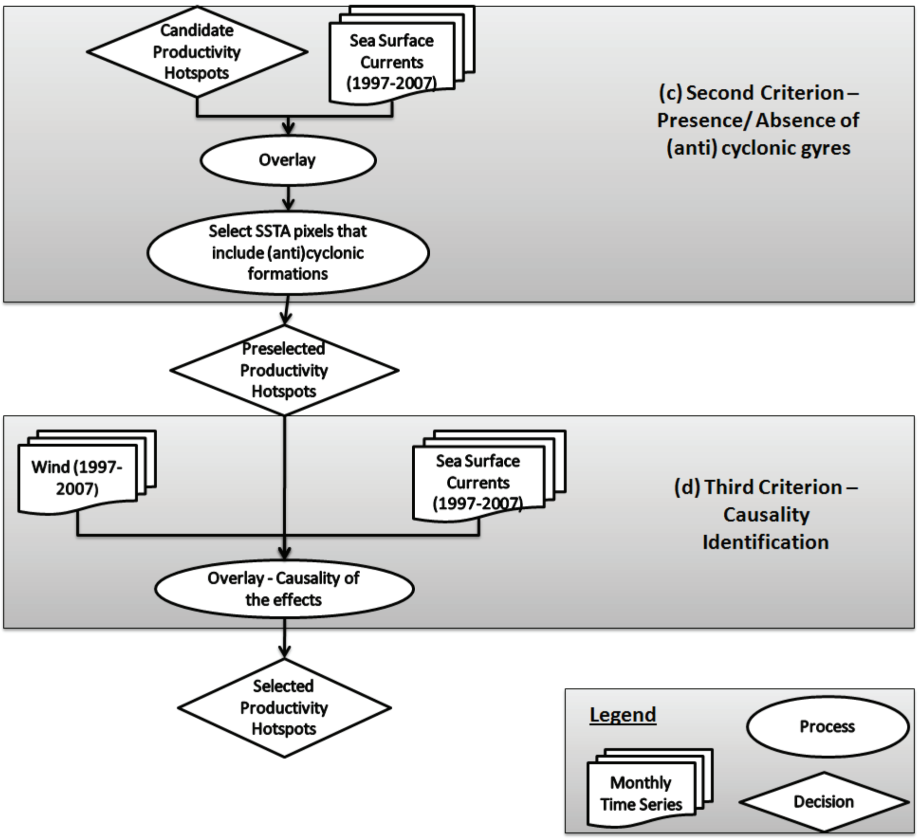

Fig.9: Second part of the followed methodology.

The last part of the analysis included the higher resolution Pearson's Product Moment Correlations between SSTA (predictor) and NDVIA and ChlaA (predictands) (Fig. 10, part e). The rainfall was excluded firstly because of lack of high resolution data and secondly because it was used as an intermediate parameter that was necessary to be investigated, in order to reveal relationships between the sea surface temperature and the vegetation variations. For the last step the highest possible resolution allowed for the correlation process from IRI/LDEO data library (IRI/LDEO Climatic Data Library, 2011) was chosen for both predictor (SSTA), 0.5x0.5 degrees lat/lon and predictands, 0.25x0.25 degrees lat/lon for the ChlaA and 0.5x0.5 degrees lat/lon for the NDVIA.

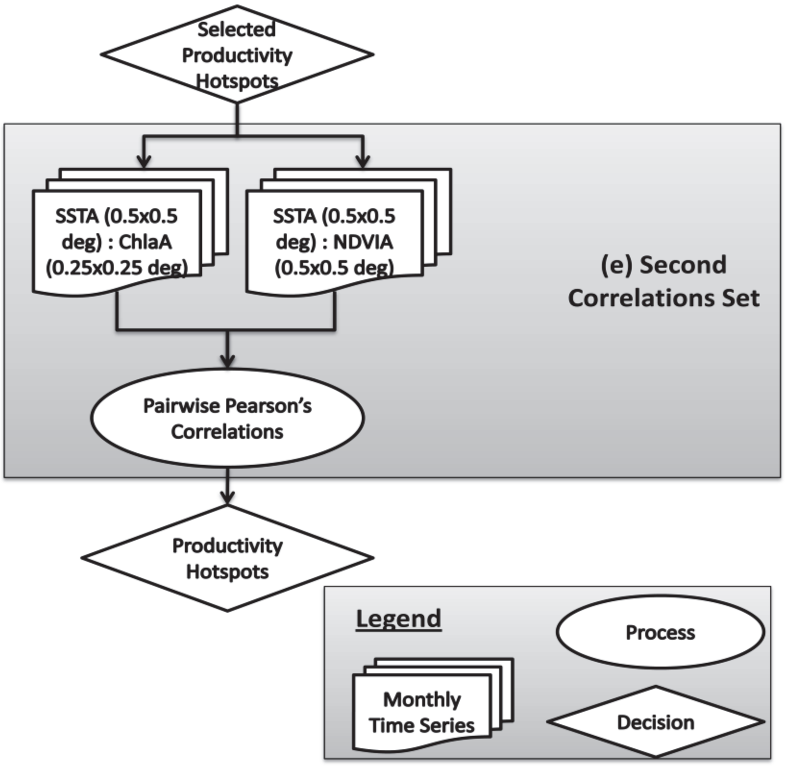

Fig.10: Third part of the followed methodology.

2.4. *Statistical Methods*

2.4.1. Normality Analysis

In statistics, the Shapiro–Wilk test tests the null hypothesis that a sample $x_1, \ldots, x_n$ came from a normally distributed population.

The test statistic is (Shapiro et al., 1965):

$$W = \frac{\left(\sum_{i=1}^{n} a_i x_{(i)}\right)^2}{\left(\sum_{i=1}^{n} (x_{(i)} - \bar{x})\right)^2} \quad \textbf{(Eq. 1)}$$

where

$x_{(i)}$ is the i^{th} order statistic, i.e., the i^{th}-smallest number in the sample;

$\bar{x}$ is the sample mean;

a_i are constants given by Equation 2 (Eq. 2).

$$(a_1 \cdots a_n) = \frac{m^T V^{-1}}{(m^T V^{-1} V^{-1} m)^{1/2}} \quad \textbf{\textit{(Eq. 2)}}$$

where

$$m = (m_1, \cdots, m_n)^T$$

and $m_1, \ldots, m_n$ are the expected values of the order statistics of independent and identically-distributed random variables sampled from the standard normal distribution, and V is the covariance matrix of those order statistics. The user may reject the null hypothesis if W is too small.

2.4.2. Correlation Analysis

The general aim of a correlation analysis is to identify the covariance of two variables and to measure the strength of any relationship between them. The correlation method that was used in this thesis is the Pearson Product-Moment Correlation.

Pearson Product-Moment Correlation illustrates the strength of the linear relationships. It is based on minimizing the sum of squares of the distances of the data points from the regression line and it is not robust for the strongly non - linear relationships and not appropriate for data that are not normally distributed (Gel et al., 2007; Kowalski, 1972). Additionally, it is sensitive to the outliers and even one extreme value can cause a considerably different result of the correlation (Baker, 1930). Regarding the skewness of the distributions it is stated that correlation results are not affected significantly by ordinary amounts of skew, but there are serious complications in the cases of much skewed distributions (Hutchinson, 1997).

The correlation coefficient (r) is bounded by -1 and 1. If the correlation is exactly -1, there is a perfect, negative linear association between the two variables, while if the correlation is exactly 1, there is a perfect, positive linear correlation. When r equals to zero, there is not any relationship between the two tested variables. Further, the square of the correlation (r^2) describes the amount of variability in one variable that is described by the other variable. Correlation does not imply causation or a physical relationship of any kind, correlations are only associated with observed instances of events.

Pearson-Product Moment Correlation coefficient (r) (Pearson, 1896, 1900) is calculated as follows:

$$r = \frac{1}{n-1}\sum_{i=1}^{n}\left(\frac{x_i-\bar{x}}{S_x}\right)\left(\frac{y_i-\bar{y}}{S_y}\right) \quad \textbf{\textit{(Eq. 3)}}$$

where:
x_i, y_i are the values of the two correlated variables
$\bar{x}, \bar{y}$ are the means of the samples
S_x, S_y are the standard deviations of the samples
i is the time (months) and
n is the number of observations (months)

Anomalies are the values above or below average and they were calculated for each variable used, separately as shown below.

$$SSTAi = (SSTi - \overline{SST}) \quad \textbf{\textit{(Eq. 4)}}$$

$$RAi = (Ri - \bar{R}) \quad \textbf{\textit{(Eq. 5)}}$$

$$NDVIAi = (NDVIi - \overline{NDVI}) \quad \textbf{\textit{(Eq. 6)}}$$

$$ChlaAi = \left(Chlai - \overline{Chla}\right) \quad \textbf{\textit{(Eq.7)}}$$

Lagged Correlations between SSTA and NDVIA, RA and ChlaA would then be:

$$\mathrm{r_{RA}} = \frac{1}{\mathrm{n}-1}\sum_{\mathrm{i}=1}^{\mathrm{n}}\left(\frac{\mathrm{SSTA_{(i-lag)}}-\overline{\mathrm{SSTA}}}{\mathrm{S_{SSTA}}}\right)\left(\frac{\mathrm{RA_i}-\overline{\mathrm{RA}}}{\mathrm{S_{RA}}}\right) \quad \textbf{\textit{(Eq. 8)}}$$

$$\mathrm{r_{NDVIA}} = \frac{1}{\mathrm{n}-1}\sum_{\mathrm{i}=1}^{\mathrm{n}}\left(\frac{\mathrm{SSTA_{(i-lag)}}-\overline{\mathrm{SSTA}}}{\mathrm{S_{SSTA}}}\right)\left(\frac{\mathrm{NDVIA_i}-\overline{\mathrm{NDVIA}}}{\mathrm{S_{NDVIA}}}\right) \quad \textbf{\textit{(Eq.9)}}$$

$$\mathrm{r_{ChlaA}} = \frac{1}{\mathrm{n}-1}\sum_{\mathrm{i}=1}^{\mathrm{n}}\left(\frac{\mathrm{SSTA_{(i-lag)}}-\overline{\mathrm{SSTA}}}{\mathrm{S_{SSTA}}}\right)\left(\frac{\mathrm{ChlaA_i}-\overline{\mathrm{ChlaA}}}{\mathrm{S_{ChlaA}}}\right) \quad \textbf{\textit{(Eq. 10)}}$$

where:
lag is the time lag for each variable
i is the time (months) and
n is the number of observations (months)

The next table shows the minimum threshold for the Pearson Correlation Coefficient (r) at a given significance level and degree of freedom(Snedecor et al., 1989).

Table 3: Critical Values of the Pearson Product Moment Correlation Coefficient for two tailed probabilities.

Level of significance (α)	*r (df=8)*
0.01	0.765
0.02	0.716
0.05	0.632

The calculation of the Pearson Product Moment Correlation Coefficient relies on the five following assumptions:

1. The variables must be either interval or ratio measurements.
2. The variables must be approximately normally distributed.
3. There is a linear relationship between the two variables.
4. Outliers are either kept to a minimum or are removed entirely.
5. There is homoscedasticity of the data.

Homoscedasticity exists in a set of data if the relationship between the X and Y variables is of equal strength across the whole range of both variables.

3. Results and Discussion

3.1. Normality Test

The result of the Shapiro-Wilk Normality Test showed that the values of all the pixels of the variables used, for all the months are normally distributed (Appendix 1, Table 1). Table 4 presents the percentage of normally distributed pixels of each variable for each month. RA presented relatively low percentage of normality, but is in almost all the months greater than 60% except July, and yet can be assumed to be a normally distributed dataset.

Table 4: Percentages of normally distributed pixels of each variable for each month used in analysis.

Month	***ChlaA (Normally distributed pixels, %)***	***NDVIA (Normally distributed pixels, %)***	***SSTA (Normally distributed pixels, %)***	***RA (Normally distributed pixels, %)***
Jan	84.0	91.2	97.5	71.3
Feb	87.3	88.5	93.8	87.4
Mar	84.3	90.9	85.0	60.1
Apr	81.5	88.8	85.0	65.7
May	89.7	91.1	100.0	65.3
Jun	85.4	93.1	100.0	60.5
Jul	90.3	88.1	93.8	54.4
Aug	85.3	89.6	98.8	62.4
Sep	84.6	88.6	91.3	66.7
Oct	84.9	84.7	100.0	70.7
Nov	85.9	85.9	85.0	73.6
Dec	80.9	88.1	97.5	84.7

According to this output the Pearson Product Moment Correlation could be used for the following analysis. Different correlation methods have been used by several studies in the past to reveal teleconnection patterns (Dragon, et al., 2010; Fontaine, et al., 2010; Huber, et al., 2011; Raicich et al., 2003). The statistical correlation methods that were selected in order to present the relationships between the three predictands (ChlaA, NDVIA and RA) and the predictor (SSTA) were presented to be significant and at first step resulted an adequate outcome illustrated in the next sections.

3.2. Candidate Productivity Hotspots

As described previously Candidate Productivity Hotspots are areas in Eastern Mediterranean that have presented significant correlation coefficients with all the three predictands that are under study (RA, NDVIA and ChlaA). Fig. 11 presents the Candidate Productivity Hotspots for each month (Fig. 6, Result of the first part of methods). The values given to the pixels of these areas are the mean absolute correlation coefficients resulted from the three correlations between predictor and predictands.

Even if the sea surface circulation criterion is not included in the analysis yet, a brief reference to the already identified by previous studies, gyral formations that could possibly coincide with the Candidate Productivity Hotspot areas is following simultaneously with the results presentation.

Generally, five distinct areas were presented in the Candidate Productivity Hotspots, the Northern, Central and Southern Aegean Sea, the Central Levantine, as well as two areas of the Eastern Levantine, the coasts of Egypt and Israel and the strait East of Cyprus Island.

These areas are territories with well studied circulation patterns as well as (anti)cyclonic formations. In terms of mesoscale activity, in Northern Aegean Samothraki Anticyclone is the dominant formation. The area was presented in the results with the highest correlation coefficients calculated for February and May.

Regarding the Southern Aegean area that is presented in the Candidate Productivity Hotspots during February, March, May and August, there has been previously recorded a multi-cyclonic system in the region for both summer and winter season (Poulos et al., 1997).

In the Central Levantine Sea a large in spatial and temporal extent area is presented in the Candidate Productivity Hotspots. It appeared in January, February, April, May and from September to November. It overlaps with the Mersa Matruh Anticyclonic area, the intensification period of which is known to be during winter months and especially in

November, while it starts generating during summer (Hamad et al., 2006).

In Eastern Levantine, an area in the Eastern strait of Cyprus presented high and significant correlation coefficients with the predictands. From September to December the effect is strong as shown in the following monthly maps (Fig. 11). In that area , the recurrent Latakia Eddie is formed (POEM group, 1992). Finally, some regions were recorded in the Southern-Eastern Levantine basin, which include small instable mesoscale formations that are small in extent and change rapidly form and position (Hamad, et al., 2006).

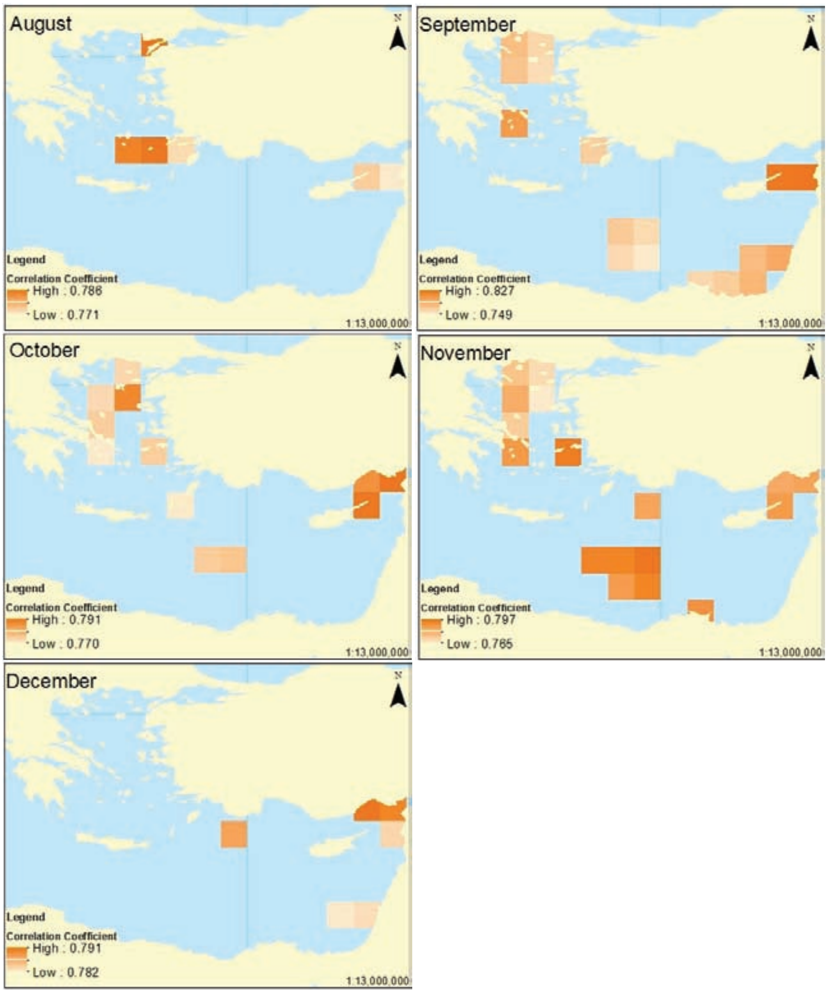

Fig.11: Averaged absolute correlation coefficients of all the three examined variables constitute the Candidate Productivity Hotspots for each month, which represented in the figure.

Generally, in Eastern Mediterranean the evaporation is largest and the SST is warmer in comparison to the rest of the basin (Sanchez-Gomez, et al., 2011). Specifically, Levantine basin presents the maximum evaporation rates and a clear seasonal cycle with minimum values in spring and maximum in fall (Romanou et al., 2010). The increased heat exchange of the basin with the atmosphere causes increased moisture and subsequently precipitation variations in European (Gimeno et al., 2010) as well as African (Rowell, 2003) regions. As described in the Introduction since there is a direct effect of the rainfall with the NDVI in the surrounding areas (Nicholson, et al., 1990), the SST is also indirectly related to vegetation. Moreover, due to the intent mesoscale formations field reported by previous studies (Amitai et al., 2010; Hamad, et al., 2006; POEM group, 1992) and taking into consideration their effects described previously, it is expected that the Eastern basin will be characterized by distinct variations in the ChlaA fields (Katara et al., 2008).

The absence of June from the Candidate Productivity Hotspots should be also noticed. An unexpected result, since during this month the Etesian winds, that drive the circulation as well as the sea-atmosphere exchanges of the area, are intensified(Poulos, et al., 1997).

The maps of Fig. 11 provide the direct answer to the first research question presenting the Candidate Productivity Hotspots and an implicit answer to the second research question, stating that the Candidate Productivity Hotspots can affect the marine and terrestrial productivity levels of the surrounding environment. As a consequence, the Null Hypothesis (H_0) of the First Hypothesis stated, which assumed that there were no effects on ChlaA, RA and NDVIA caused from areas of Eastern Mediterranean, was rejected.

3.3. Selected Productivity Hotspots

The definition of Preselected Productivity Hotspots was an intermediate step in order to get the Selected Productivity Hotspots. This step included the overlay of the Candidate Productivity Hotspots (presented in previous section 3.2.) with the monthly sea surface currents of all the years separately. Additionally, the (anti)cyclonic formations should be identified and overlap with the Candidate Productivity Hotspots for at least seven out of ten years of the study period (Appendix I, Table 2).This fulfilled the second criterion regarding the presence of the gyral formations (Fig. 9, part (c)).

Since from this step on the terminology that will be used for the rest of the report will be in terms of (anti)cyclonic gyral areas, Fig. 12 presents the four anticyclonic gyres and their locations that were resulted to be Preselected Productivity Hotspots in Eastern Mediterranean (Fig. 9, part (c)).

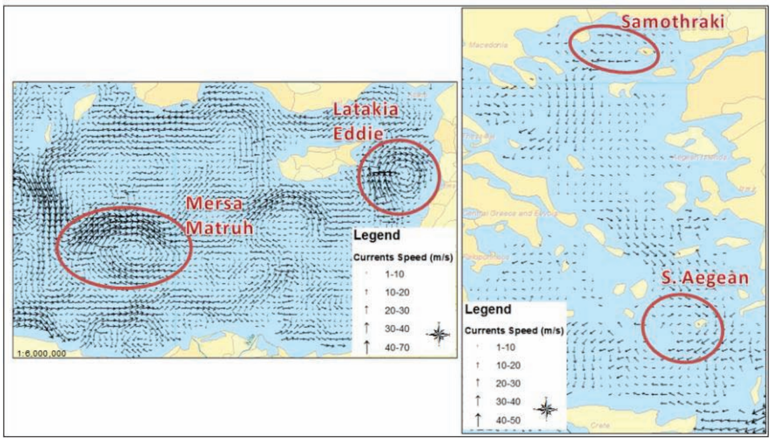

Fig.12: Location of the Preselected Productivity Hotspots in Aegean Sea (right image) and Levantine Basin (left image).
Mersa Matruh Anticyclone and Latakia Eddie in Levantine Basin, Samothraki Anticyclone in Northern Aegean Sea and Southern Aegean Anticyclone.

The averaged absolute correlation coefficients resulted from the correlations between SSTA and ChlaA-RA-NDVIA of the Preselected Productivity Hotspots areas were plotted (Fig. 13) in order to present numerically those relations.

The highest correlation coefficients (over 0.82) were presented on January with 6 months time lags for ChlaA in the Mersa Matruh area and the Latakia Eddie area and on September and October without time lag for RA in the Latakia Eddie area. Most of the averaged absolute correlation coefficients are in the range between 0.76 and 0.82. Both anticyclones that presented the higher correlation coefficients are the largest in spacial extent and strongest in terms of currents velocities. The first characteristic, the spatial extent, could possibly explain the high RA and NDVIA correlation coefficients due to the dependency of those variables on the evaporation of the area, while the second, the currents velocities, could be the reason of the gyres' effects on Chla variations.

Regarding the time lags, in January-February and June ChlaA showed the highest delays, but for the rest months, correlations without time lag were the strongest. NDVIA seems to follow the same pattern with RA by presenting the same or higher time lag. NDVIA in most cases had two or three months lag, while RA responded faster on SSTA and presented zero to one month time lags.

A remark regarding the Preselected Productivity Hotspots is that the gyres formations that are included in their areas are just clockwise anticyclonic formations. As mentioned in the Introduction, those gyres have warm cores, act like nutrient traps (Biggs, 1992) and present increased Chla blooms on their boundary areas(Raj, et al., 2010) as well as enhance the productivity of higher levels (Dragon, et al., 2010), mechanisms which can possibly explain their strong influences on local as well as remote regions.

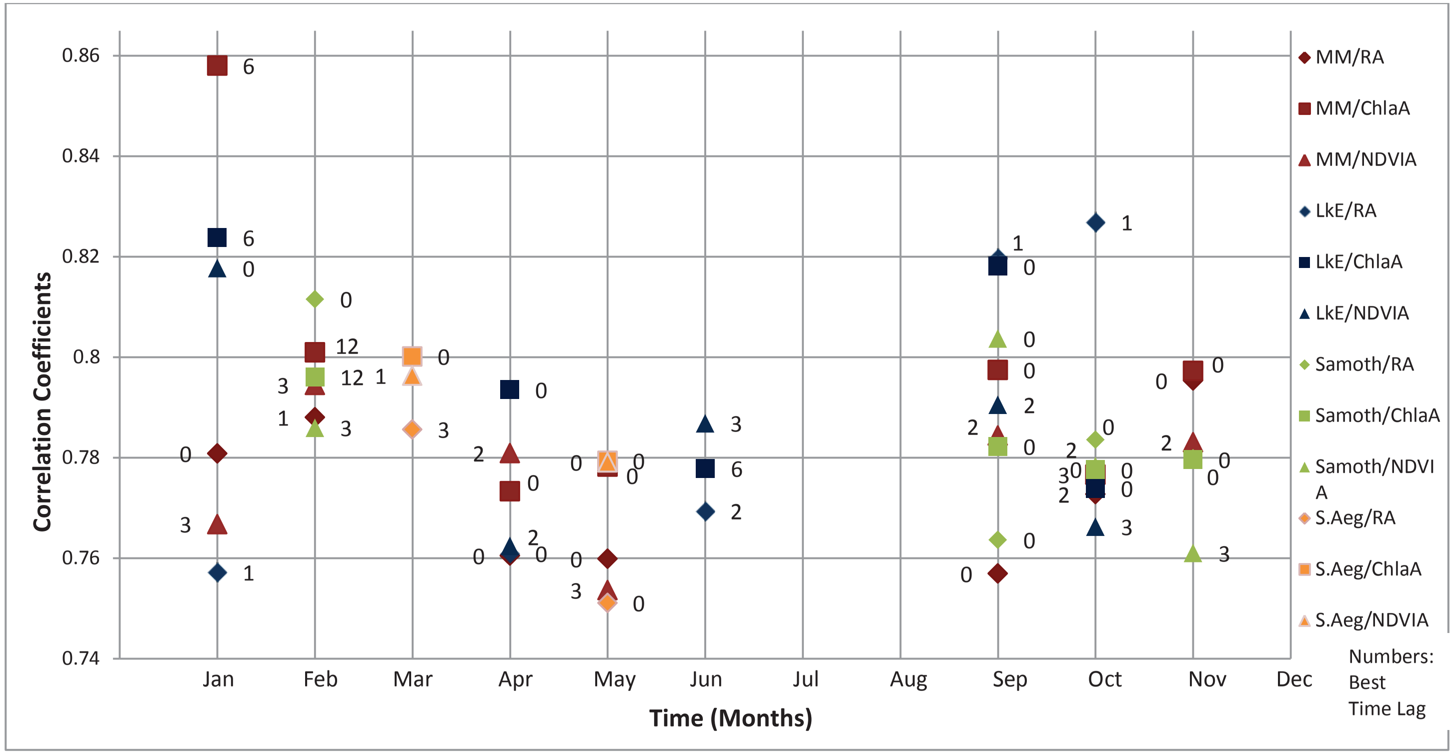

Fig.13: Graphical representation of the absolute mean Correlation Coefficients of each month and each anticyclonic area of Eastern Mediterranean.
(MM = Mersa Matruh, LkE = Latakia Eddie, Samoth = Samothraki Anticyclone and S.Aeg = Southern Aegean Anticyclone).

Results and Discussion

The term Selected Productivity Hotspots as described in the "Terminology" section includes the areas of Preselected Productivity Hotspots, which resulted after the fulfilment of the criterion regarding the presence/absence of the (anti)cyclonic gyres, as well as the identification of the causality based on the wind and the sea surface currents conditions at the affecting and the affected areas.

Despite the intent gyral field developing in the Eastern Mediterranean basin, just two anticyclonic areas was chosen to be the Selected Productivity Hotspots.

The first area is located at 28° - 29°E and 33°N in the Central Levantine Basin, includes the Mersa Matruh Anticyclone and presented to be a Selected Productivity Hotspot in April (Appendix II, Fig 1), in May (Appendix II, Fig 2) and in October as well (Fig. 14).In those Figures the Mersah Matruh Anticyclone is presented by the currents velocity vectors that reveal the circulation pattern in one month. The orange coloured area denotes the Selected Productivity Hotspot and the value of each pixel is the average absolute correlation coefficient of all the three predictands (RA, NDVIA and ChlaA).

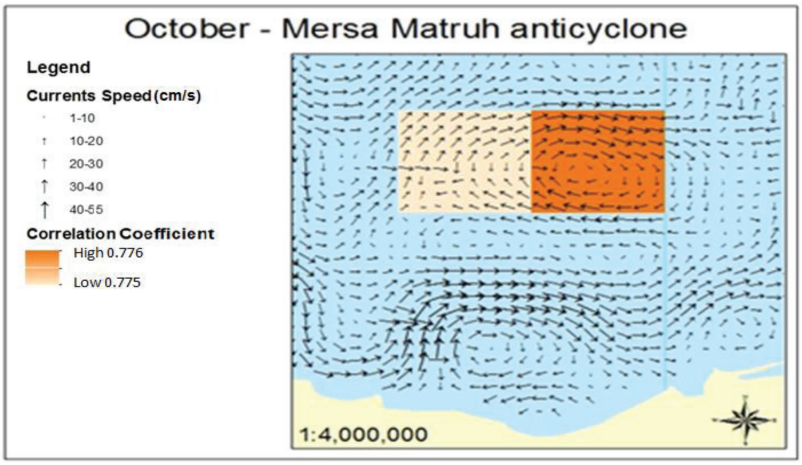

Fig.14: Average absolute correlation coefficients of Selected Productivity Hotspot in October, including the Mersa Matruh Anticyclone indicated by the currents velocity vectors in the area.

The second area that fulfilled the causality criterion and became a Selected Productivity Hotspot is located in the Northern Aegean Sea at 24° - 25°E and 40°N, which includes the Samothraki Anticyclone within its boundaries (Fig. 15).

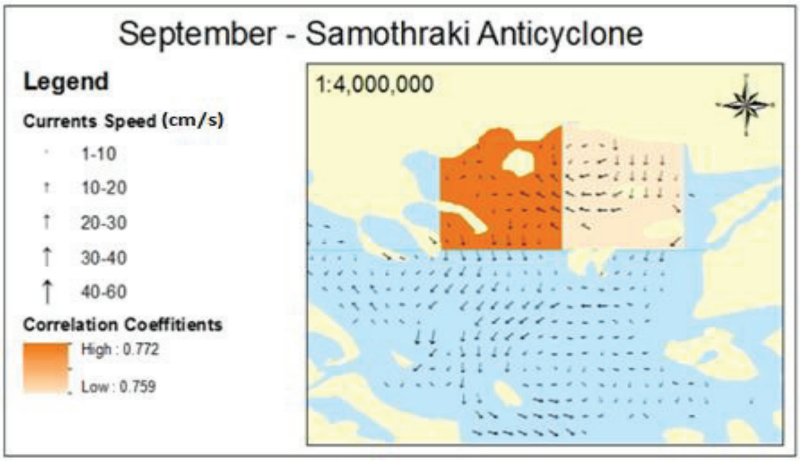

Fig.15: Average absolute correlation coefficient of Selected Productivity Hotspot in September, including the Samothraki Anticyclone indicated by the currents velocity vectors in the area.

Mersa Matruh Anticyclone is the major feature in Eastern Mediterranean that affects both marine and terrestrial Primary Productivity elsewhere. It is recorded to be the strongest mesoscale feature with a maximum diameter of 250-350 km (Golnaraghi, 1993). It propagates spatially between 26-30°E and 32-34.5°N and temporally starts generating during summer and reaches its strongest and largest extent during October-November (Hamad, et al., 2006). Due to its spatial and temporal extent as well as the intensified current velocity field and the strong winds of the area which increase the evaporation rates, Mersa Matruh Anticyclone is the main outcome from this analysis. As expected, this warm, anticyclonic core presented high correlations with RA and subsequently NDVIA for the selected months and a strong effect on the ChlaA on its boundaries as well as the studied marine area. Further, during winter Mid Mediterranean Jet flows along its northern boundary (Korres et al., 2003) and seems to affect its high correlations with the three parameters examined (ChlaA-RA-NDVIA).

Samothraki Anticyclone is the second gyre that was revealed from the analysis, propagating in North Aegean Sea. This gyre is described as permanent and important feature of a rather complex region (Zervakis et al., 2002). Black Sea Water (BSW) outflow from Dardanelles strait is the principal water mass that reaches the anticyclonic area and affects its physical and biological conditions. BSW is characterised by increased secondary nutrient concentration (such as organic nitrogen and carbon) (Siokou-Frangou et al., 2002), low salinity and temperature (Sylaios, 2011; Zervakis, et al., 2002). It is assumed that the gyre increases the BSW residence time in the

North Aegean, thus favouring the local productivity levels (Sylaios, 2011). Additionally, the Aegean Sea is losing heat from the surface layers (Poulos, et al., 1997) and specifically North Aegean, in seasonal scale, gains heat during spring and summer and start losing it in September (Zervakis, et al., 2002).

An unexpected result was the absence of the permanent and strong formations, like Ierapetra Anticyclone, Pelops Anticyclone, Shikmona Anticyclone as well as the Rhodes Cyclone that develop in the Levantine basin. The signal of those gyres was clear when the circulation of the area was examined. A possible explanation of this outcome is the overlapping effect of all the three predictands used in this study and characterises the Selected Productivity Hotspots. For example, Rhodes cyclone is considered to be the largest cold core of the Eastern Mediterranean which means that, according to the cyclonic mechanism, should cause increase of Primary Production. On the contrary, this cold mass of water is expected to present reduced evaporation, which leads to absence of correlation with RA and NDVIA. Additionally, regarding the anticyclonic formations most probably their smaller extend than Mersa Matruh or possible lower correlations coefficients than the critical values could be the reasons for their absence, which on the other hand enhances the importance of the results of this study and the strong impact of Mersa Matruh and Samothraki Anticyclones.

Finally, this section provides the answer to the third Research Question formed in this study regarding the Selected Productivity Hotspots that are presented to affect both marine and terrestrial Primary Productivity levels, the causality of these effects could be indicated and, also, included (anti)cyclonic gyres within their boundaries.

3.4. Productivity Hotspots and their effects on productivity indicators

The last step of the correlation analysis included the pair-wise Pearson Product Moment Correlations between SSTA and ChlaA and NDVIA, similarly to the first correlations set, but with higher spatial resolution. The resolution used for SSTA and NDVIA was 0.5x0.5 degrees and for ChlaA 0.25x0.25 degrees lat/lon. From those correlations the Productivity Hotspots (Fig. 10, Result of third part of the methods) were chosen as well as the marine and terrestrial areas that they affect regarding the Primary Productivity.

Maps of Productivity Hotspots are presented combined with their effects on the productivity indicators (ChlaA and NDVIA) in separate sections for marine and terrestrial productivity. The highlighted regions in each map show the areas that were directly influenced by the Productivity Hotspots as well as the corresponding identified cause of the relationships. For the sake of brevity, just the maps of the effects of Mersa Matruh in October as well as Samothraki gyre in September will be presented and explained in detail in these sections, while the rest maps and additional explanations can be found in the Appendix III. These two cases where selected because they were representative for both anticyclonic areas resulted from the analysis and also, specifically Mersa Matruh in October, presented the highest correlation coefficients among the other months.

3.4.1. Impacts on Marine Productivity

Direct and indirect connections were identified in the correlation analysis between SSTA in Mersa Matruh and Samothraki Anticyclones during April, May and October for the former and September for the latter.

The SSTA in Mersa Matruh Anticyclone against ChlaA in the Mediterranean basin is presented in October (Fig. 16), April (Appendix III, Fig. 1) and May (Appendix III, Fig. 2). Regarding the direct effects, Mersa Matruh resulted to be highly important for the surrounding marine area, the Levantine basin. In addition, indirect effects with remote areas were identified. The gyre appeared to be connected with marine areas in Aegean, Ionian, Adriatic, Tyrrhenian, Balearic and Alboran Seas in the different months. The zero time lag makes direct connections impossible and reveals possible existing teleconnections.

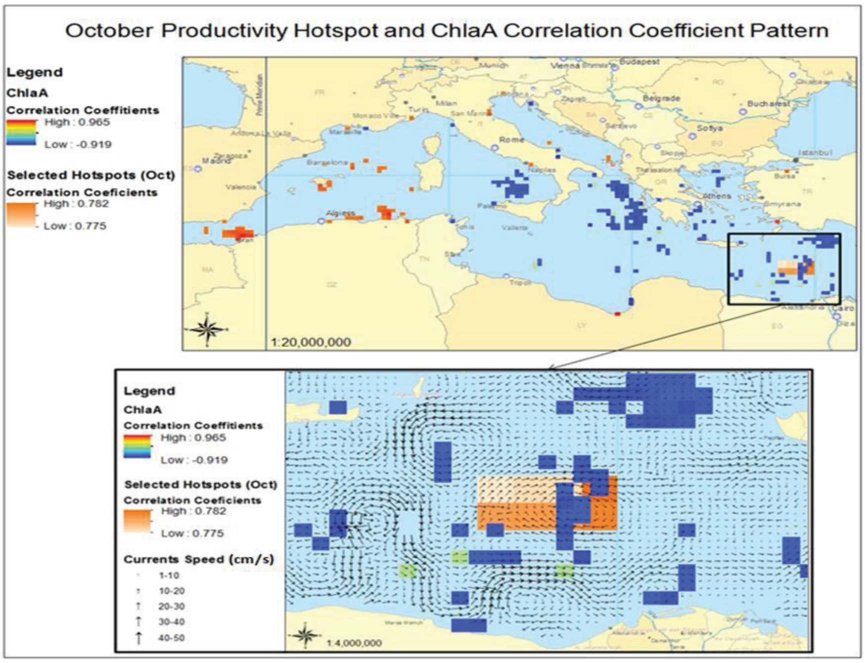

Fig.16: Productivity Hotspot in October (Mersa Matruh Anticyclone) and the average ChlaA Correlation Coefficient pattern in the Mediterranean Sea (upper image).
Highlighted is the Final Productivity Hotspot area with the currents velocity vectors and the average ChlaA Correlation Coefficients.

The result of the correlation of the SSTA in Samothraki Anticyclonic area against ChlaA is presented in Fig. 17, including the circulation of the study area in September. SSTA in Samothraki region presented high and negative correlation coefficients with the whole Aegean Sea as well as the Western and Central Levantine Sea.

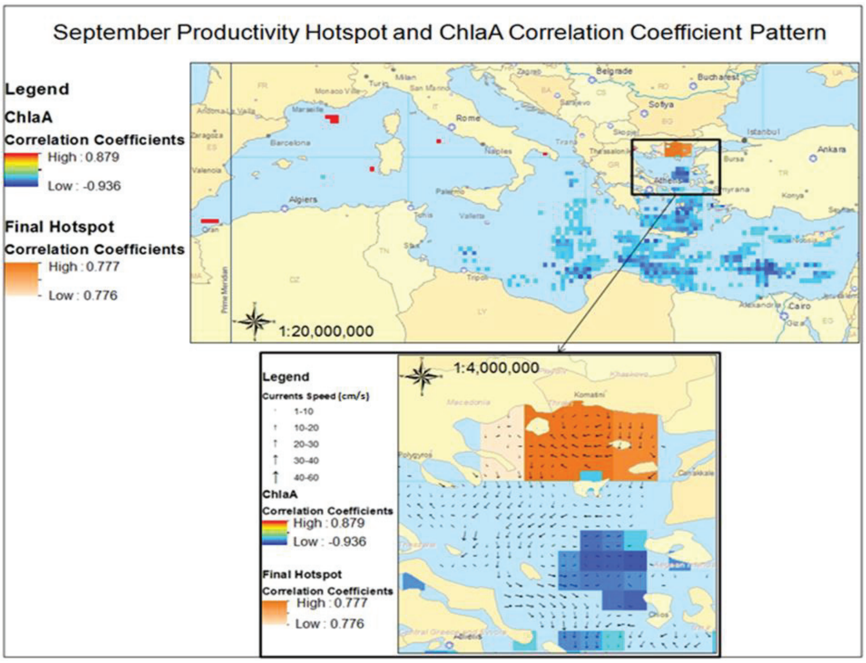

Fig.17: Final Productivity Hotspot in September (Samothraki Anticyclone) and the average ChlaA Correlation Coefficient pattern in the Mediterranean Sea (upper image).
Highlighted is the Final Productivity Hotspot area with the currents velocity vectors and the average ChlaA Correlation Coefficients.

The next two paragraphs discuss the direct effects first of Mersa Matruh Anticyclone and second of the Samothraki Anticyclone with the surrounding areas, providing evidence for the identified causality of the relations. The converse relation between SST and Chla concentration in the sea can explain the negative correlation coefficients presented in the results. The higher the temperature of surface water in the anticyclonic area is, the lower the chlorophyll is expected to be (Biggs, 1992). Based on the circulation pattern of the Levantine and Aegean regions, the direct negative relationships revealed can be partly justified.

Mersa Matruh appears to be one of the considerable features that affect the Chla patterns of Eastern Mediterranean even if it cannot be assumed that is the only one. In October (Fig. 16) the main direct effect is presented in a large area on its North-eastern part. Following the Mid Mediterranean Jet a branch of water is moving towards the Northern-Eastern part of Mersa Matruh to reach that region. Additionally, the currents move towards the Egyptian coasts and affect also negatively the Chla concentrations of the area. Branches of water appear to connect Mersa Matruh with other gyral formations of the sub-basin, like the ones presented in Ierapetra Anticyclonic and Rhodes Cyclonic region. An additional expected effect of the anticyclone is its influence on the Chla in its core, which can be an indicator for possible warmer than average temperatures in the centre of the gyre during October.

The second identified gyre was Samothraki gyre that is developing in the North Aegean, as described in the previous section (section 3.3). The main characteristic of the area is the surface BSW outflow. As mentioned, Samothraki Anticyclone increases the residence time of the cold, brackish, high in nutrients and of low salinity BSW in the North Aegean region. An increasing trend of oligotrophy has been recorded from the Northern to the Southern Aegean regarding the autotrophic plankton (Ignatiades et al., 2002; Siokou-Frangou, et al., 2002) which can be an indicator of the Chla concentrations. It could be assumed that the BSW increases the productivity levels in the Northern Aegean and especially in the boundaries of the Samothraki gyre (Isari et al., 2006) but as the water mass remains in the area and also is moving towards the Southern part of the basin the nutrients for the primary production are being consumed and followed by the simultaneous increase of the SST it influence the Southern part negatively in terms of Primary Productivity.

Except the identified direct impacts of the two anticyclonic gyres there have been revealed several indirect, remote connections which cannot have an apparent and noticeable explanation. SSTA in Mersa Matruh Anticyclone presented the highest negative correlations with ChlaA in October. They are present in the Aegean, Ionian and Tyrrhenian Seas. Additionally there were positive correlations with the Western Mediterranean sub-basins. In regard to indirect relations of Samothraki Anticyclone, it presented high negative correlations with the whole Levantine as well as the Southern Aegean Sea. These teleconnections depict the Mediterranean dipole of SST studied previously (Skliris et al., 2012) and reveal possible dependency of the mesoscale phenomena studied here from larger scale phenomena.

Several previous studies have described the sea-atmosphere interactions (Katara, et al., 2008; Lolis et al., 2002) and usually in relation to larger scale, distant atmospheric and oceanic phenomena (Fontaine, et al., 2010; Josey et al., 2011; Katara et al., 2011; Skliris, et al., 2012; Ziv et al., 2006). In this way, correlations of Mediterranean Sea parameters with North Atlantic Oscillation (NAO) in decadal scale (Skliris, et al., 2012), with Eastern Atlantic (EA) pattern (Josey, et al., 2011) and Mediterranean Oscillation (MO) (Katara, et al., 2011) have been identified. In the results of this study an underlying connection of Mersa Matruh and Samothraki Anticyclones with these larger scale phenomena could be assumed. The results seem to agree with Skliris et. al. (2012) that showed significant correlation of the NAO with Mediterranean SST on decadal scale, revealing that the negative phase of NAO, which lasted from 1990's until mid-2000's, is associated with warmer SSTs in Eastern Mediterranean and with lower SSTs in the Western basin. The same authors identified higher SST warming rates in Eastern Mediterranean basin and on the contrary lower rates in the western basin after 1990. Regarding the EA pattern, that shows similar cycle with NAO in annual scale, its positive phase could be related to above-average SSTs in the whole Mediterranean basin (Josey 2011) and leads to stronger water exchange between Western Mediterranean and EA (Katara 2011). Additionally, this positive phase has been recorded that lasted from late 1970's till mid - 2000's. Considering the negative relation of SSTA-ChlaA concentration, the anticorrelated SSTA in Mersa Matruh and Samothraki Anticyclones with ChlaA in Central and Eastern Mediterranean basins during the spring (April-May) and autumn (September-October) in the decade 1997-2007,it could be assumed that both gyral formations are possibly driven by these larger scale phenomena and the variations of SSTA in their cores could provide a general picture of the temperature anomalies of the basin. An additional teleconnection is revealed in October Final Productivity Hotspot's outcome; the positive correlation of the Mersa Matruh gyre with the Western part of Mediterranean, which can possibly explain the stronger EA colder water inflow in the Mediterranean during a strong positive phase of EA pattern that could cause above-average Chla concentrations and the below-average SSTs of Western Mediterranean due to the negative phase of NAO during this decade. Furthermore, this outcome agrees with a negative MO, in which the temperatures are presented to be higher in the Eastern Mediterranean and lower to the Western Mediterranean basin. The exact mechanisms of those teleconnections are not yet known and it would be rather complex to be explained from this thesis.

3.4.2. Impacts on Terrestrial Productivity

Teleconnections were identified in the correlation analysis between SSTA in Mersa Matruh and Samothraki Anticyclones and NDVIA during April, May, October and September.

The SSTA in Mersa Matruh Anticyclone against NDVIA in the Mediterranean region is presented in October (Fig. 18), April (Apendix III, Fig. 3) and May (Apendix III, Fig. 4) and high coefficients presented in regions of Algeria, Spain and Israel, respectively. The wind field revealed the identified causality of the relationships as well there were similar correlation results between SSTA and RA presented in the area. The rest of the regions had to be rejected. Even if the wind pattern seems to explain the possible causality, the SSTA-RA correlations could not reveal any potential effects on the rainfall variations.

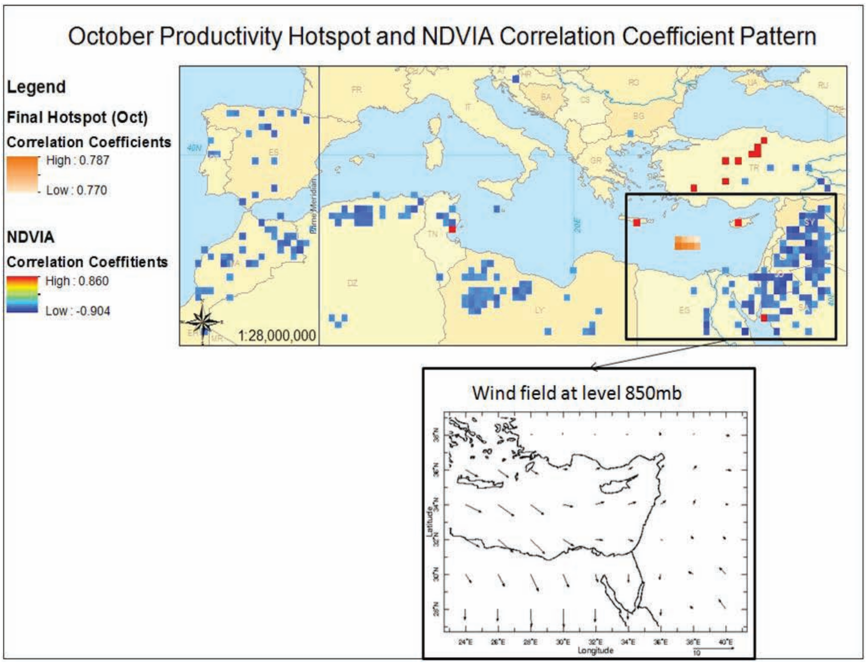

Fig.18: Final Productivity Hotspot in October (Mersa Matruh Anticyclone) and the average NDVIA Correlation Coefficient pattern around the Mediterranean Sea (upper image).
Highlighted are the wind velocity vectors of the area of interest.

Teleconnections of the SSTA at Northern Aegean, the Samothraki gyre area, with NDVIA in Algeria were found (Fig. 19). The corresponding RA- SSTA correlation showed equivalent results in the same area. Additionally, there was a zero time lag for this connection, which can be associated with the very strong atmospheric swirl that was developed in the area during September.

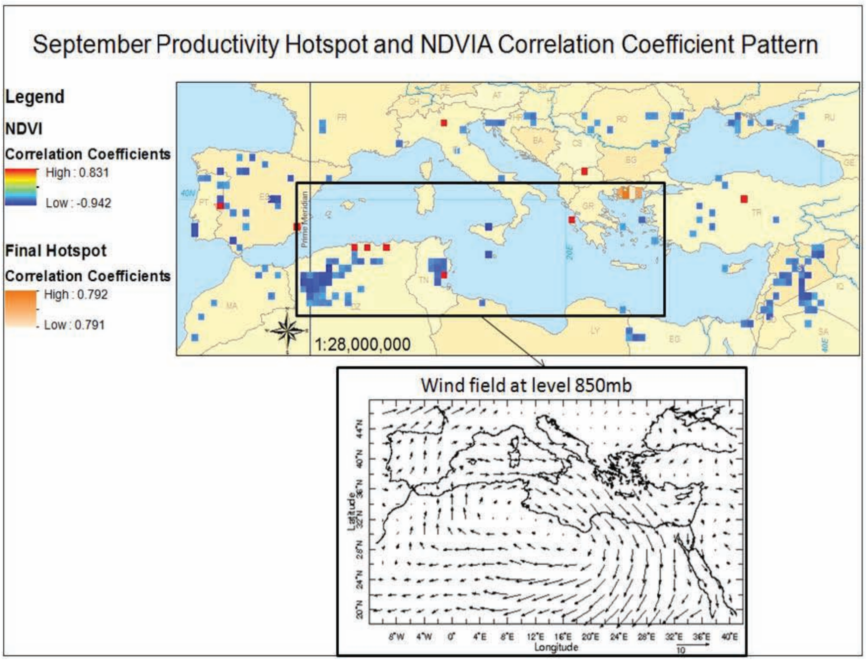

Fig.19: Final Productivity Hotspot in September (Samothraki Anticyclone) and the average NDVIA Correlation Coefficient pattern around the Mediterranean Sea (upper image).
Highlighted are the wind velocity vectors of the area of interest.

According to the results of previous studies the increase of SST of Eastern Mediterranean Sea causes increased evaporation that enhances the moisture content of the air and the atmospheric advection as well as the rainfall (Rowell, 2003) and NDVI (Huber, et al., 2011) to the African Sahel. The results of the present analysis show an inverse negative effect of the SSTA in E. Mediterranean on the northern coasts of Africa in Algeria, Spanish regions and Israel.

The Northern regions of Algeria are characterized by hot summers and mild, wet winters and dominated by moist Mediterranean and Atlantic winds (Touchan et al., 2011). The precipitation in the area and more specifically for the last years the drought of the area is highly associated with warm tropical Atlantic SST and the Atlantic tripole (S. L. Li et al., 2003) as well as the North Atlantic Oscillation (Xoplaki et al., 2004). During September the wind pattern reveals a clockwise swirl of the atmospheric circulation named Libya anticyclone (Baldi et al., 2006) that is presented to be the reason of the correlation between the SSTA Samothraki Anticyclone and the Algerian regions. A possible mechanism causing this relation, when positive SSTA is presented, could be the transfer on the one hand of the moisture from the Eastern Mediterranean to the Algerian regions by Libyan anticyclone, but on the other hand this leads to warm advection (Lolis, et al., 2002) and transfers the moisture further towards the Alps, where it causes abundant rainfalls (Baldi, et al., 2006). In agreement with that, the correlation process revealed positive correlation coefficients of SSTA in Samothraki against RA in the Alps region during September, but it was in the order of 0.6-0.7 and not significantly enough to be included in the effects of the studied gyre. This mechanism could cause drought events in the Algerian regions studied here. On the contrary, when negative SSTA is presented in Samothraki area during September, respectively, rainfall evens can be observed in Algerian regions. The same atmospheric formation seems to be the reason of the effects of Mersa Matruh gyre on vegetation in Algeria in April (Appendix III, Fig. 3) and in Spain in May (Appendix III, Fig. 4).

The area of Israel and Lebanon present a clear seasonal cycle in rainfall; wet period is from October to March and the dry period is until September (Ben-Gai et al., 1998). The precipitation of the area as described in previous studies is influenced by larger scale phenomena, such as El Nino (Price et al., 1998), NAO and EA jet (Dunkeloh et al., 2003), as well as hurricanes (Hurricane Olga) (Alpert et al., 2005). One of the possible mechanisms that could explain the primary relation of the SSTA in Mersa Matruh gyre with the RA and secondarily with the NDVIA is the cold advection (Ziv, et al., 2006). This advection occurs above the warm Eastern Mediterranean water and causes precipitation instability over Israel and Lebanon. As wind moves above the sea it gets moisturised as well as colder in comparison to the land. As it is continues moving towards the Eastern coasts of Mediterranean it creates a low pressure field in the area of Israel (Ziv, et al., 2006), it causes vertical advection of the moisture to the higher atmospheric layers and results strong precipitation events. The two months lag in the RA-SSTA correlation indicates that lower (higher) than normal SSTs in the Mersa Matruh area during August can cause high (low) precipitation during October and higher (lower) vegetation growth during November. Even if these explanations given here could describe some connections at a satisfactory level, further investigation of direct/indirect relations with global atmospheric phenomena is necessary in order to give a possible complete picture of the system.

3.5. Error Propagation

The first uncertainty of this research is the "natural uncertainty" which explains the randomness of the environmental and biological systems (Isukapalli et al., 2001). In this thesis several parameters like the ocean evaporation or important components of the heat fluxes (solar radiation, sensible heat) (Poulos, et al., 1997) were avoided due to the time and complexity limitations. Moreover, the assumptions taken regarding the homogeneity and the linear relations between the variables used add more uncertainty to the results.

Further the coarse spatial as well as temporal resolution may introduce an uncertainty in the results. On the other hand, data used in this study demonstrate sufficient variability which can be used to explain the processes at this scale.

Finally, one highly important uncertainty source is the data set uncertainty which in this case propagates through the correlation and mathematically there is a summation of those errors included in each of the resulting correlation coefficients calculation. Data sets are characterized by different errors and uncertainties, depending on their collection strategies and sources. In some cases, where for instance merged datasets including buoys, satellite data, gauged data or numerical modeling results, the combined error is difficult to be calculated (Xie et al., 1996).

4. Conclusions and Recommendations

4.1. Conclusions

New teleconnection patterns between anticyclonic gyral formations and marine and terrestrial primary productivity have been discovered in this study. In Mediterranean Sea the mesoscale (anti)cyclonic field is very intense, thus it was expected it would influence the primary productivity in both marine and terrestrial environment, in local and regional scale. Among all, just two anticyclonic gyres, named Mersa Matruh and Samothraki Anticyclones were identified as the most important ones. Mersa Matruh is located in the Levantine basin and its SSTA presented high significant correlation coefficients with all the examined variables (ChlaA, RA and NDVIA) during April, May and October. Samothraki gyre is located in Northern Aegean Sea and appeared to influence the surrounding environment during September.

Mersa Matruh Anticyclone presented negative impacts on the marine and terrestrial primary production elsewhere. Regarding the marine environment it had negative influence on the Chla in the Eastern Mediterranean sub-basins during all the months and positive effect on Western Mediterranean basin during October. As a direct effect can be concluded that the above average SSTs in this large anticyclonic area causes below average Chla concentrations and results a lower primary production rates. As an indirect effect and with agreement to larger scale phenomena variations (NAO, EA pattern), SSTA in the Mersa Matruh Anticyclone can indicate the SST variations of both Mediterranean sub-basins for each month resulted. In the terrestrial environment it presented negative correlations during all the mentioned months, but in different areas. In April affected NDVI in Algeria, in May the effects were present in Spain and during October in Israel and Lebanon. Each time different atmospheric circulation as well as wind speed appeared to drive these teleconnections.

Samothraki Anticyclone presented negative impacts on the marine and terrestrial primary production in September, elsewhere as well. Its SSTA presented negative correlations with the ChlaA in the Central as well as the Southern Aegean and Levantine sub-basin. Due to the special characteristic of the area, Samothraki gyre seems to contribute in a large extent to its Primary Productivity directly. Even if its core consist of the cold BSW and presents cold temperatures, it still presents negative effects on the ChlaA, fact that could be explained from the higher primary productivity levels inside the Samothraki Anticyclonic core as well as the increase of the residence time of the BSW in the North Aegean. Additionally, it could indirectly represent the SSTA variations of the sub-basins mentioned above as a response to larger scale phenomena, like NAO or EA pattern. Regarding the terrestrial environment Samothraki gyre was teleconnected with the vegetation of Algeria and a wind swirl developed in the area during September gives the possible explanation of this connection.

The use of the online platform of IRI/LDEO Data Library and the Ingrid Programming Language for the completion of the analyses appeared to be a very beneficial tool. It provided easy and real- time data access, monitoring and processing of them and it is indeed a promising application for future research. Additionally, the assumption that the earth is the best model of itself, since this was the main logic behind this research, resulted to be sensible.

Taking into consideration the importance of primary productivity, it is a necessity to investigate possible environmental parameters that are influencing it either locally or remotely. Despite that this research is a first step for the teleconnectivity of the (anti)cyclonic gyres with primary productivity elsewhere; it is also a step for the further understanding of the environmental system.

4.2. Recommendations

Considering the complexity of the system a first recommendation would be the investigation of more variables that could affect and provide details for the teleconnections of the gyral formations. Datasets like moisture fluxes, atmospheric pressure as well as land surface temperature could give a different picture of the mechanisms causing the impacts on terrestrial production. On the other hand, sea surface height and sea surface salinity and additional data from underlying water layers could be useful marine variables in order to distinguish as much as possible the different water masses and their origin. In addition, more specific teleconnections of those gyres with larger scale phenomena would be interesting to be investigated, as for example the exact correlation of important gyres like Mersa Matruh and Samothraki Anticyclones with NAO, EA pattern and MO indexes.

Furthermore, higher temporal and spacial resolution would provide more accurate results in terms of areal segregation. By using higher spacial resolution the differences between the characteristics of the cores of gyral formations would be more distinct and they could be isolated from the surrounding waters more accurately. The higher temporal resolution could provide a clearer picture of the developing cycle of the gyres during a month; a weekly or 10-days resolution would be favourable.

In this study the effects of the SST in the specific gyral areas on remote rainfall, marine and terrestrial primary productivity where studied. It would be of high interest the investigation of the opposite effects of rainfall on the SST and the Chla concentrations, or the effects of river outflows to the marine production and how could this affect the subsequent teleconnections.

Finally the Mediterranean region was an ideal study area, but a investigation of the (anti)cyclonic gyres of the larger gyral systems of the global ocean could give some important information for the climate and possible predictive mechanisms for the climate variations.

Chapter 4

References

Agresti, A., & Coull, B. A. (1998). Approximate Is Better than "Exact" for Interval Estimation of Binomial Proportions. *The American Statistician, 52*(2), 119-126.

Alhammoud, B., Béranger, K., Mortier, L., Crépon, M., & Dekeyser, I. (2005). Surface circulation of the Levantine Basin: Comparison of model results with observations. *Progress In Oceanography, 66*(2-4), 299-320.

Alpert, P., Price, C., Krichak, S. O., Ziv, B., Saaroni, H., Osetinsky, I., et al. (2005). Tropical tele-connections to the Mediterranean climate and weather. *Advances in Geosciences, 2*, 157-160.

Amitai, Y., Lehahn, Y., Lazar, A., & Heifetz, E. (2010). Surface circulation of the eastern Mediterranean Levantine basin: Insights from analyzing 14 years of satellite altimetry data. *J. Geophys. Res., 115*(C10), pages: C10058.

AVISO Web Site. (1997 - 2011). Retrieved 13/06/2011, from http://www.aviso.oceanobs.com/en/home/index.html

Baker, G. A. (1930). The Significance of the Product-Moment Coefficient of Correlation with Special Reference to the Character of the Marginal Distributions. *Journal of the American Statistical Association, 25*(172), 387-396.

Baldi, M., & Dalu, G. A. (2006). *Geopotential oscillations and rainfall cycle in the Mediterranean Region.* Paper presented at the 6th Annual Meeting of European Meteorological Society (EMS), Ljubljana, Slovenia.

Belkin, I. M., Cornillon, P. C., & Sherman, K. (2009). Fronts in Large Marine Ecosystems. *Progress In Oceanography, 81*(1-4), 223-236.

Ben-Gai, T., Bitan, A., Manes, A., Alpert, P., & Rubin, S. (1998). Spatial and temporal changes in rainfall frequency distribution patterns in Israel. *Theoretical and Applied Climatology, 61*(3-4), 177-190.

Beuvier, J., Sevault, F., Herrmann, M., Kontoyiannis, H., Ludwig, W., Rixen, M., et al. (2010). Modeling the Mediterranean Sea interannual variability during 1961 - 2000: Focus on the Eastern Mediterranean Transient. *J. Geophys. Res., 115*(C8), C08017.

Bigg, G. R., Jickells, T. D., Liss, P. S., & Osborn, T. J. (2003). The role of the oceans in climate. *International Journal of Climatology, 23*(10), 1127-1159.

Biggs, D. C. (1992). Nutrients, Plankton and Productivity in a Warm-Core Ring in the Western Gulf of Mexico. *Journal of Geophysical Research-Oceans, 97*(C2), 2143-2154.

References

Bost, C. A., Cotte, C., Bailleul, F., Cherel, Y., Charrassin, J. B., Guinet, C., et al. (2009). The importance of oceanographic fronts to marine birds and mammals of the southern oceans. *Journal of Marine Systems, 78*(3), 363-376.

Boyce, D. G., Lewis, M. R., & Worm, B. (2010). Global phytoplankton decline over the past century. *Nature, 466*(7306), 591-596.

Bridgman, H., & Oliver, J. E. (Eds.). (2006). *The Global Climate System. Patterns, Process and Teleconnections.*: Cambridge University Press.

Cartes, J. E., Maynou, F., Abello, P., Emelianov, M., de Sola, L. G., & Sole, M. (2011). Long-term changes in the abundance and deepening of the deep-sea shrimp Aristaeomorpha foliacea in the Balearic Basin: Relationships with hydrographic changes at the Levantine Intermediate Water. *Journal of Marine Systems, 88*(4), 516-525.

Columbia University. (2011). The International Research Institute for Climate and Society (IRI). Retrieved September 2011, from Columbia University http://iridl.ldeo.columbia.edu/index.html

Department of Oceanography Naval Postgraduate School. (2010). http://www.oc.nps.edu/. Retrieved 10-August-2011

Dragon, A.-C., Monestiez, P., Bar-Hen, A., & Guinet, C. (2010). Linking foraging behaviour to physical oceanographic structures: Southern elephant seals and mesoscale eddies east of Kerguelen Islands. *Progress In Oceanography, 87*(1-4), 61-71.

Dunkeloh, A., & Jacobeit, J. (2003). Circulation dynamics of Mediterranean precipitation variability 1948-98. *International Journal of Climatology, 23*(15), 1843-1866.

Fontaine, B., Garcia-Serrano, J., Roucou, P., Rodriguez-Fonseca, B., Losada, T., Chauvin, F., et al. (2010). Impacts of warm and cold situations in the Mediterranean basins on the West African monsoon: observed connection patterns (1979-2006) and climate simulations. *Climate Dynamics, 35*(1), 95-114.

Freeman, E. A., & Moisen, G. (2008). PresenceAbsence: An R package for presence absence analysis. *Journal of Statistical Software, 23*(11), 1-31.

Garcia-Gomez, M., & Maestre, F. T. (2011). Remote sensing data predict indicators of soil functioning in semi-arid steppes, central Spain. *Ecological Indicators, 11*(5), 1476-1481.

Gel, Y. R., Miao, W., & Gastwirth, J. L. (2007). Robust directed tests of normality against heavy-tailed alternatives. *Computational Statistics & Data Analysis, 51*(5), 2734-2746.

Gerin, R., Poulain, P. M., Taupier-Letage, I., Millot, C., Ben Ismail, S., & Sammari, C. (2009). Surface circulation in the Eastern

Mediterranean using drifters (2005-2007). *Ocean Science, 5*(4), 559-574.

Gimeno, L., Drumond, A., Nieto, R., Trigo, R. M., & Stohl, A. (2010). On the origin of continental precipitation. *Geophysical Research Letters, 37*(L13804), doi:10.1029/2010GL043712

Golnaraghi, M. (1993). Dynamical Studies of the Mersa-Matruh gyre - Intense meander and ring formation events. *Deep-Sea Research Part Ii-Topical Studies in Oceanography, 40*(6), 1247-1267.

Hamad, N., Millot, C., & Taupier-Letage, I. (2006). The surface circulation in the eastern basin of the Mediterranean Sea. *Scientia Marina, 70*(3), 457-503.

Hátún, H., Payne, M. R., Beaugrand, G., Reid, P. C., Sandø, A. B., Drange, H., et al. (2009). Large bio-geographical shifts in the north-eastern Atlantic Ocean: From the subpolar gyre, via plankton, to blue whiting and pilot whales. *Progress In Oceanography, 80*(3-4), 149-162.

Hatzaki, M., Flocas, H. A., Maheras, P., Asimakopoulos, D. N., & Giannakopoulos, C. (2005). Study of future climatic variations of a teleconnection pattern affecting Eastern Mediterranean. In T. D. Lekkas (Ed.), *Proceedings of the 9th International Conference on Environmental Science and Technology, Vol A - Oral Presentations, Pts A and B* (pp. A567-A572). Athens: Univ Aegean.

Huber, S., & Fensholt, R. (2011). Analysis of teleconnections between AVHRR-based sea surface temperature and vegetation productivity in the semi-arid Sahel. *Remote Sensing of Environment, 115*(12), 3276-3285.

Hutchinson, T. P. (1997). A Comment on Correlation in Skewed Distributions. *The Journal of General Psychology, 124*(2), 211-215.

Ignatiades, L., Psarra, S., Zervakis, V., Pagou, K., Souvermezoglou, E., Assimakopoulou, G., et al. (2002). Phytoplankton size-based dynamics in the Aegean Sea (Eastern Mediterranean). *Journal of Marine Systems, 36*(1-2), 11-28.

IRI/LDEO Climatic Data Library. (2011). Ingrid Function Documentation. Retrieved September 2011, from Columbia University http://iridl.ldeo.columbia.edu/dochelp/Documentation/

Isada, T., Hattori-Saito, A., Saito, H., Ikeda, T., & Suzuki, K. (2010). Primary productivity and its bio-optical modeling in the Oyashio region, NW Pacific during the spring bloom 2007. *Deep-Sea Research Part Ii-Topical Studies in Oceanography, 57*(17-18), 1653-1664.

References

Isari, S., Ramfos, A., Somarakis, S., Koutsikopoulos, C., Kallianiotis, A., & Fragopoulu, N. (2006). Mesozooplankton distribution in relation to hydrology of the Northeastern Aegean Sea, Eastern Mediterranean. *Journal of Plankton Research, 28*(3), 241-255.

Isukapalli, S., & Georgopoulos, D. (2001). Computational Methods for Sensitivity and Uncertainty Analysis for Environmental and Biological Models. Triangle Park, NC 27711: National Exposure Research Laboratory Office of Research and Development U.S. Environmental Protection Agency Research.

Josey, S. A., Somot, S., & Tsimplis, M. (2011). Impacts of atmospheric modes of variability on Mediterranean Sea surface heat exchange. *Journal of Geophysical Research-Oceans, 116*.

Karydis, M. (2009). Eutrophication Assessment of Coastal Waters Based on Indicators: A Literature Review. *Global Nest Journal, 11*(4), 373-390.

Katara, I., Illian, J., Pierce, G. J., Scott, B., & Wang, J. J. (2008). Atmospheric forcing on chlorophyll concentration in the Mediterranean. *Hydrobiologia, 612*, 33-48.

Katara, I., Palialexis, A., Wang, J., Scott, B., Illian, J., Valavanis, V., et al. (2011). Oceanic patterns in the Mediterranean: Are they influenced by teleconnection patterns? . *International Journal of Climatology, In review*.

Kirono, D. G. C., Chiew, F. H. S., & Kent, D. M. (2010). Identification of best predictors for forecasting seasonal rainfall and runoff in Australia. *Hydrological Processes, 24*(10), 1237-1247.

Korres, G., & Lascaratos, A. (2003). A one-way nested eddy resolving model of the Aegean and Levantine basins: implementation and climatological runs. *Annales Geophysicae, 21*(1), 205-220.

Kowalski, C. J. (1972). Effects of Non-Normality on Distribution of Sample Product-Moment Correlation Coefficient. *Journal of the Royal Statistical Society Series C-Applied Statistics, 21*(1), 1-&.

Lebeaupin, C., Ducrocq, V., & Giordani, H. (2006). Sensitivity of torrential rain events to the sea surface temperature based on high-resolution numerical forecasts. *Journal of Geophysical Research-Atmospheres, 111*(D12), doi:10.1029/2005JD006541.

Legendre, L., & Watt, W. D. (1970). Distribution of Primary Production relative to a cyclonic gyre in Baie-Des-Chaleurs. *Marine Biology, 7*(2), 167- 170.

Li, L. Z. X. (2006). Atmospheric GCM response to an idealized anomaly of the Mediterranean sea surface temperature. *Climate Dynamics, 27*(5), 543-552.

Li, S. L., Robinson, W. A., & Peng, S. L. (2003). Influence of the north Atlantic SST tripole on northwest African rainfall. *Journal of Geophysical Research-Atmospheres, 108*(D19).

Lolis, C. J., Bartzokas, A., & Katsoulis, B. D. (2002). Spatial and temporal 850 hPA air temperature and sea-surface temperature covariances in the Mediterranean region and their connection to atmospheric circulation. *International Journal of Climatology, 22*(6), 663-676.

Lolis, C. J., Bartzokas, A., & Katsoulis, B. D. (2004). Relation between sensible and latent heat fluxes in the Mediterranean and precipitation in the Greek area during winter. *International Journal of Climatology, 24*(14), 1803-1816.

Marullo, S., Santoleri, R., Malanotte-Rizzoli, P., & Bergamasco, A. (1999). The sea surface temperature field in the Eastern Mediterranean from advanced very high resolution radiometer (AVHRR) data - Part I. Seasonal variability. *Journal of Marine Systems, 20*(1-4), 63-81.

Maselli, F., Chiesi, M., Moriondo, M., Fibbi, L., Bindi, M., & Running, S. W. (2009). Modelling the forest carbon budget of a Mediterranean region through the integration of ground and satellite data. *Ecological Modelling, 220*(3), 330-342.

Matsoukas, C., Banks, A. C., Hatzianastassiou, N., Pavlakis, K. G., Hatzidimitriou, D., Drakakis, E., et al. (2005). Seasonal heat budget of the Mediterranean Sea. *Journal of Geophysical Research-Oceans, 110*(C12).

McGill University. (2003). Thermal Advection. Retrieved 31/01, 2012, from http://www.meteo.mcgill.ca/wxlab/ATOC-546/notes/lesson09.thermal_advection/

Menna, M., & Poulain, P. M. (2010). Mediterranean intermediate circulation estimated from Argo data in 2003-2010. *Ocean Science, 6*(1), 331-343.

Munyati, C., & Ratshibvumo, T. (2011). Characterising vegetation cover in relation to land use in the Inkomati catchment, South Africa, using Landsat imagery. *Area, 43*(2), 189-201.

Nicholson, S. E., Davenport, M. L., & Malo, A. R. (1990). A comparison of the vegetation responce to rainfall in the Sahel and East- Africa, using Normalized Difference Vegetation Index from NOAA AVHRR. *Climatic Change, 17*(2-3), 209-241.

Pearson, K. (1896). Mathematical Contributions to the Theory of Evolution. III. Regression, Heredity, and Panmixia. *Philosophical Transactions of the Royal Society of London. Series A, Containing Papers of a Mathematical or Physical Character, 187*, 253-318.

Pearson, K. (1900). On the criterion that a given system of deviations from the probable in the case of a correlated system of variables is such that it can reasonably be supposed to have arisen in a random sampling. *Philosophical Magazine, 5*, 157-175.

Philippon, N., Jarlan, L., Martiny, N., Camberlin, P., & Mougin, E. (2007). Characterization of the interannual and intraseasonal variability of West African vegetation between 1982 and 2002 by means of NOAA AVHRR NDVI data. *Journal of Climate, 20*(7), 1202-1218.

POEM group. (1992). General circulation of the Eastern Mediterranean. *Earth-Science Reviews, 32*(4), 285-309.

Poulos, S. E., Drakopoulos, P. G., & Collins, M. B. (1997). Seasonal variability in sea surface oceanographic conditions in the Aegean Sea (Eastern Mediterranean): an overview. *Journal of Marine Systems, 13*(1–4), 225-244.

Price, C., Stone, L., Huppert, A., Rajagopalan, B., & Alpert, P. (1998). A possible link between El Nino and precipitation in Israel. *Geophysical Research Letters, 25*(21), 3963-3966.

Raicich, F., Pinardi, N., & Navarra, A. (2003). Teleconnections between Indian monsoon and Sahel rainfall and the Mediterranean. *International Journal of Climatology, 23*(2), 173-186.

Raj, R. P., Peter, B. N., & Pushpadas, D. (2010). Oceanic and atmospheric influences on the variability of phytoplankton bloom in the Southwestern Indian Ocean. *Journal of Marine Systems, 82*(4), 217-229.

Romanou, A., Tselioudis, G., Zerefos, C. S., Clayson, C. A., Curry, J. A., & Andersson, A. (2010). Evaporation-Precipitation Variability over the Mediterranean and the Black Seas from Satellite and Reanalysis Estimates. *Journal of Climate, 23*(19), 5268-5287.

Rowell, D. P. (2003). The Impact of Mediterranean SSTs on the Sahelian Rainfall Season. *Journal of Climate, 16*(5), 849-862.

Said, M. A., Gerges, M. A., Maiyza, I. A., Hussein, M. A., & Radwan, A. A. (2011). Changes in Atlantic Water characteristics in the south-eastern Mediterranean Sea as a result of natural and anthropogenic activities. *Oceanologia, 53*(1), 81-95.

Sanchez-Gomez, E., Somot, S., Josey, S., Dubois, C., Elguindi, N., & Déqué, M. (2011). Evaluation of Mediterranean Sea water and heat budgets simulated by an ensemble of high resolution regional climate models. *Climate Dynamics, 37*(9), 2067-2086.

Shapiro, S. S., & Wilk, M. B. (1965). An Analysis of Variance Test for Normality (Complete Samples). *Biometrika, 52*(3/4), 591-611.

Siokou-Frangou, I., Bianchi, M., Christaki, U., Christou, E. D., Giannakourou, A., Gotsis, O., et al. (2002). Carbon flow in the planktonic food web along a gradient of oligotrophy in the Aegean Sea (Mediterranean Sea). *Journal of Marine Systems, 33–34*(0), 335-353.

Siokou-Frangou, I., Christaki, U., Mazzocchi, M. G., Montresor, M., d'Alcala, M. R., Vaque, D., et al. (2010). Plankton in the open Mediterranean Sea: a review. *Biogeosciences, 7*(5), 1543-1586.

Skliris, N., Sofianos, S., Gkanasos, A., Mantziafou, A., Vervatis, V., Axaopoulos, P., et al. (2012). Decadal scale variability of sea surface temperature in the Mediterranean Sea in relation to atmospheric variability. *Ocean Dynamics, 62*(1), 13-30.

Snedecor, G. W., & Cochran, W. G. (1989). *Statistical Methods*. Ames,Iowa: Iowa State University Press, Blackwell Publishing Professional

Su, W., Sun, Z. P., Li, D. L., Ramsankaran, R., Zhu, X., & Guo, X. Y. (2009). Vegetation recovery monitoring over the waste dump in Haizhou opencast coalmine area, China, during 1975-2000 using NDVI and VF index. *Journal of the Indian Society of Remote Sensing, 37*(4), 631-645.

Sylaios, G. (2011). Meteorological influences on the surface hydrographic patterns of the North Aegean Sea. *Oceanologia, 53*(1), 57-80.

Touchan, R., Anchukaitis, K. J., Meko, D. M., Sabir, M., Attalah, S., & Aloui, A. (2011). Spatiotemporal drought variability in northwestern Africa over the last nine centuries. *Climate Dynamics, 37*(1-2), 237-252.

USGS. (2012, 27/12/2011). The Water Cycle. Retrieved 21/01/2012, from http://ga.water.usgs.gov/edu/watercycle

Velaoras, D., & Lascaratos, A. (2010). North-Central Aegean Sea surface and intermediate water masses and their role in triggering the Eastern Mediterranean Transient. *Journal of Marine Systems, 83*(1-2), 58-66.

Xie, P. P., & Arkin, P. A. (1996). Analyses of global monthly precipitation using gauge observations, satellite estimates, and numerical model predictions. [Article]. *Journal of Climate, 9*(4), 840-858.

Xoplaki, E., Gonzalez-Rouco, J. F., Luterbacher, J., & Wanner, H. (2004). Wet season Mediterranean precipitation variability: influence of large-scale dynamics and trends. *Climate Dynamics, 23*(1), 63-78.

Zervakis, V., & Georgopoulos, D. (2002). Hydrology and circulation in the North Aegean (Eastern Mediterranean) throughout 1997 and 1998. *Mediterranean Marine Science, 3/1*, 5-19.

Zhou, L. T. (2011). Interdecadal change in sea surface temperature anomalies associated with winter rainfall over South China.

Journal of Geophysical Research-Atmospheres, 116, pages: D11101.
Ziv, B., Dayan, U., Kushnir, Y., Roth, C., & Enzel, Y. (2006). Regional and global atmospheric patterns governing rainfall in the southern Levant. *International Journal of Climatology, 26*(1), 55-73.

Appendices

Appendix I

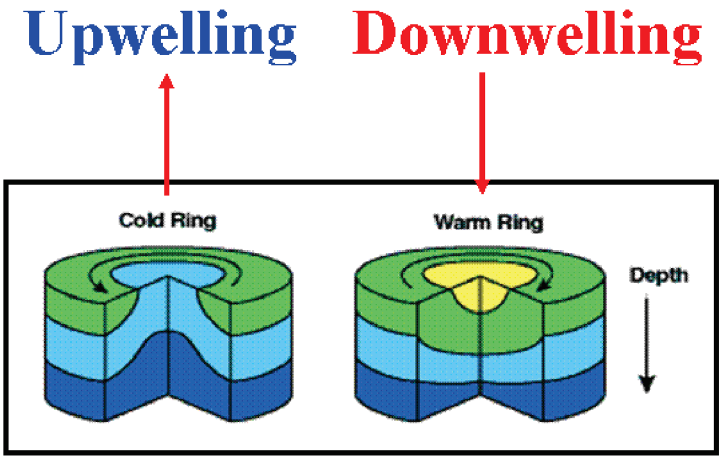

Fig.1: Representation of cyclonic (upwelling) and anticyclonic (downwelling) formations. Source: www.oc.nps.navy.mil (Department of Oceanography Naval Postgraduate School, 2010)

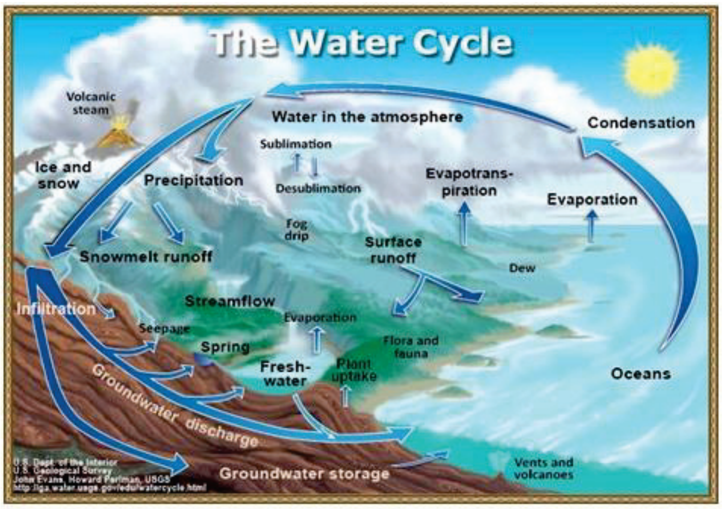

Fig. 2: Water cycle summary. The main processes underlying behind this research are the Ocean Evaporation, the Precipitation and the Plant uptake. Source: USGS website (USGS, 2012).

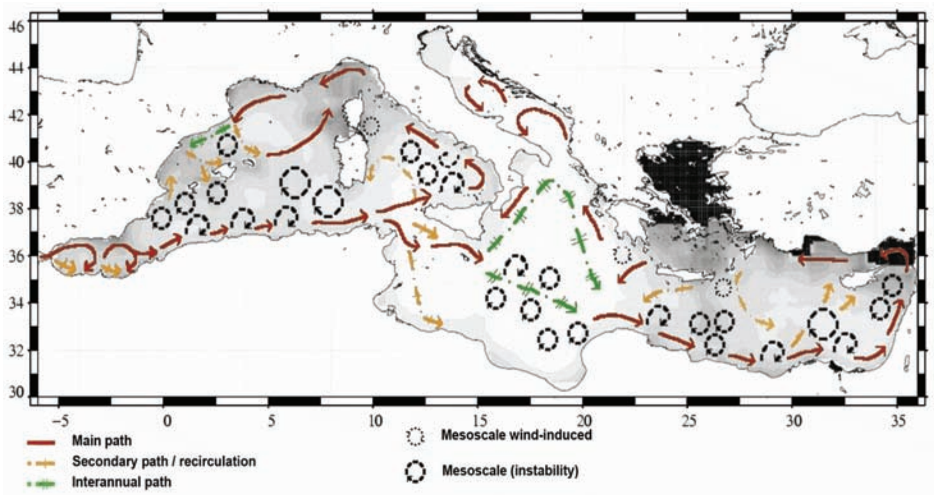

Fig. 3: Description of the general circulation of the Mediterranean Sea. Source: www.aviso.oceanobs.com(AVISO Web Site, 1997 - 2011).

Numerous previous researches have been carried out for the Mediterranean circulation patterns, but the eastern basin has not been explored as much as the western. In the eastern Mediterranean basin the circulation studies revealed significant seasonal and annual oceanographic phenomena by using different methods. Satellite tracked drifters have been used by Gerin et al. (2009) to describe the basin's surface circulation patterns. Statistical analyses of satellite altimetry time series have been used in order to represent the eddies in Eastern Mediterranean Sea (Amitai, et al., 2010), which described the Mid Mediterranean Jet that flows eastwards, transports the AW into the basin and generates the two long-term formations of Mersa-Martuh and Shikmona anticyclones as well as the seasonal, because of the Etesian winds, presence of Ierapetra Anticyclone. Additionally, Hamad et al. (2006) have used SST datasets in order to investigate the eastern Mediterranean circulation as well, which described for example, the record of the wind-induced Pelops Anticyclone and the Lybio-Egyptian Eddies created by the AW current that flows towards the east. Model simulations have been also applied for the this study area (Alhammoud et al., 2005) and revealed the main patterns of the basin (such as AW flow, Mersa Matruh Anticyclone Shikmona Anticyclone) but still were not able to reproduce some mesoscale formations (like Ierapetra Anticyclone). The presence of those major (anti)cyclonic formations extending in this relatively small basin can create unique, but rather complex, biological, physical and ecological regimes.

Table 1: Example table resulted from Matlab process for the Shapiro-Wilk Normality Test. The first column presents the actual result, zero represents the normally distributed pixel (null hypothesis accepted) and one the not normal pixels (null hypothesis rejected). Additionally W and P-values were shown and finally the X and Y coordinates of each pixel examined.

SW result	**W**	**P-value**	**X**	**Y**
1	0.022101	0.809888	20.5	39.5
0	0.054603	0.849862	20.5	38.5
0	0.541245	0.943704	20.5	37.5
0	0.51936	0.936928	20.5	36.5
0	0.284234	0.91705	20.5	35.5
0	0.895651	0.970523	20.5	34.5
0	0.126124	0.878713	20.5	33.5
0	0.310903	0.914173	20.5	32.5
1	0.048229	0.844546	21.5	38.5
.				
.				
.				
0	0.256614	0.906313	28.5	34.5
0	0.847529	0.96562	28.5	33.5
0	0.133709	0.880921	28.5	32.5
0	0.732124	0.955375	28.5	31.5
1	0.014366	0.789756	29.5	40.5
0	0.341569	0.918123	29.5	36.5
0	0.43265	0.928432	29.5	35.5
0	0.388349	0.923644	29.5	34.5
0	0.480779	0.933266	29.5	33.5
0	0.532541	0.938143	29.5	32.5
0	0.596646	0.943855	29.5	31.5

Table 2: Months that identified (anti)cyclonic formations coincided with Candidate Productivity Hotspots.

Months/Gyres	*Mersa Matruh Anticyclone*	*Samothraki Anticyclone*	*South Aegean Cyclones*	*Latakia Eddie*
Jan	9	-	-	7
Feb	10	8	-	-
Mar	-	-	7	-
Apr	10	-	-	7
May	10	-	7	-
Jun	-	-	-	9
Jul	-	-	-	-
Aug	-	-	-	-
Sep	9	7	-	7
Oct	9	8	-	8
Nov	10	8	-	-
Dec	-	-	-	-

Appendix II

Selected Productivity Hotspots

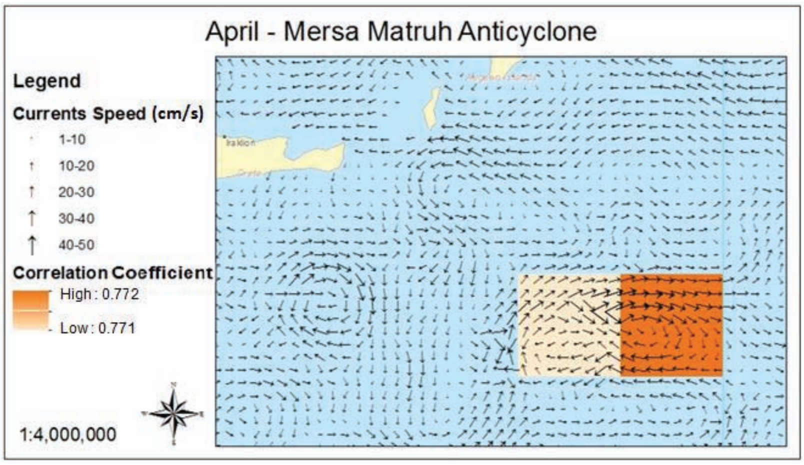

Fig. 1: Averaging of absolute correlation coefficients of Selected Productivity Hotspot in April, including the Mersa Matruh Anticyclone indicated by the currents velocity vectors in the area.

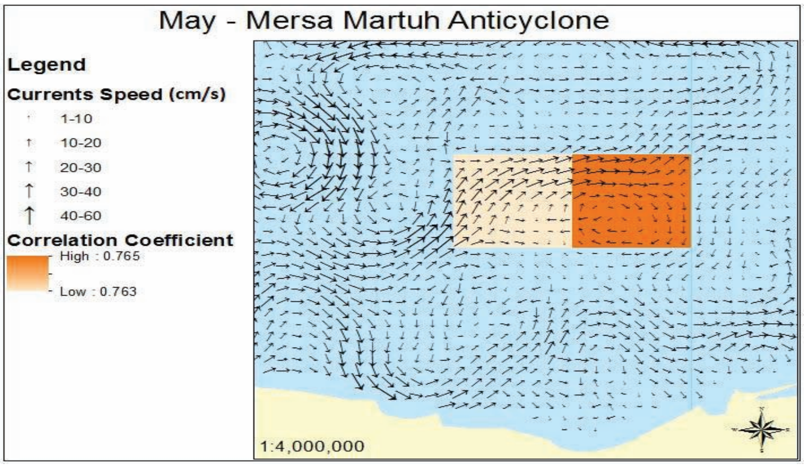

Fig. 2: Average absolute correlation coefficients of Selected Productivity Hotspot in May, including the Mersa Matruh Anticyclone indicated by the currents velocity vectors in the area.

Appendix III

Productivity Hotspots

Effects in Marine Productivity

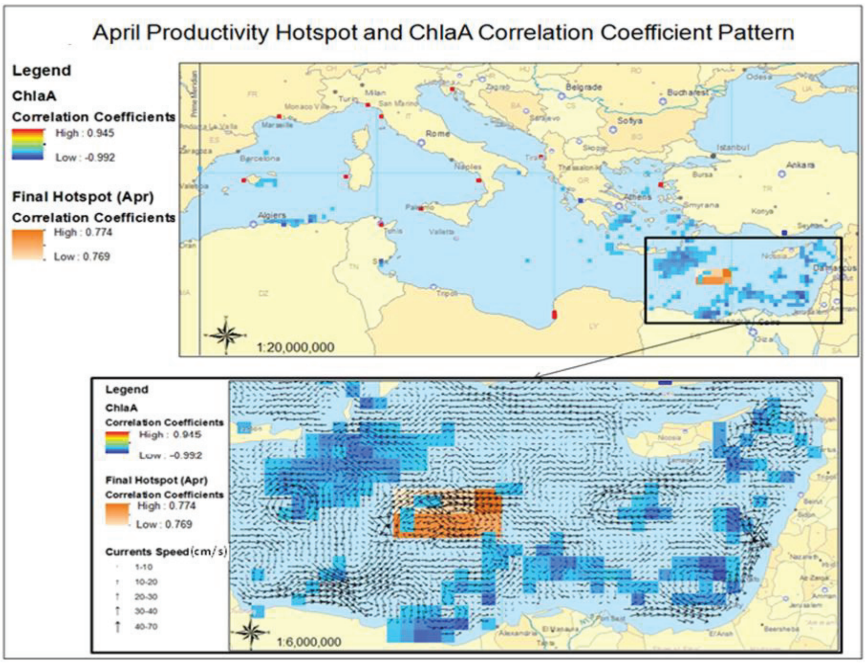

Fig. 1: Productivity Hotspot in April (Mersa Matruh Anticyclone) indicated by the mean correlation coefficients for each pixel and the average ChlaA Correlation Coefficient pattern in the Mediterranean Sea (upper image). Highlighted is the Final Productivity Hotspot area with the currents velocity vectors and the average ChlaA Correlation Coefficients.

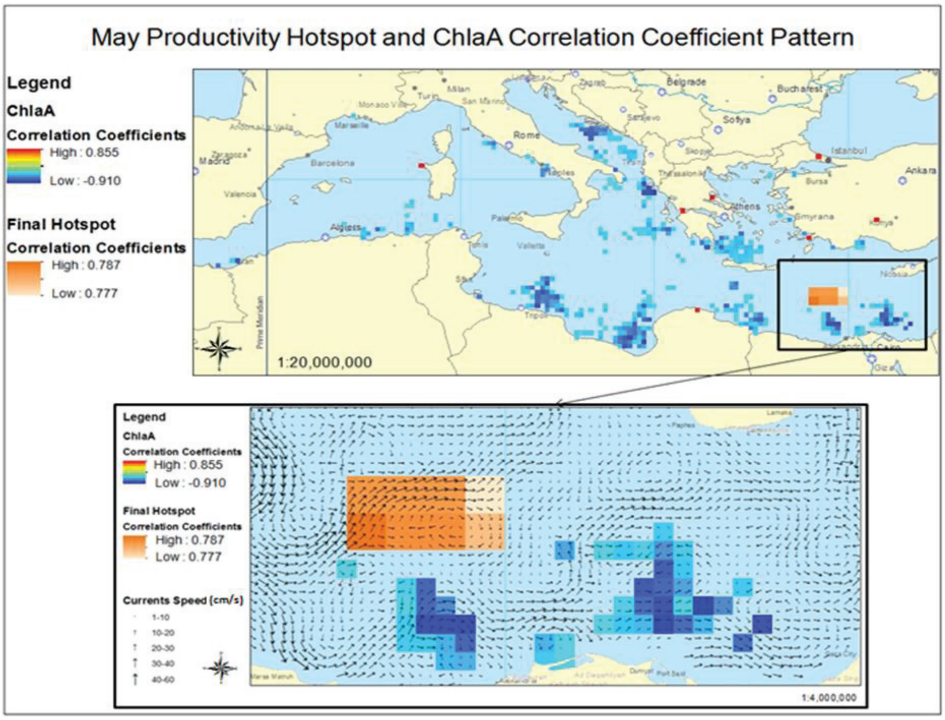

Fig. 2: Productivity Hotspot in May (Mersa Matruh Anticyclone) and the average ChlaA Correlation Coefficient pattern in the Mediterranean Sea (upper image). Highlighted is the Final Productivity Hotspot area with the currents velocity vectors and the average ChlaA Correlation Coefficients.

In April (Fig. 1) it is presented to affect directly other gyral areas as well, such as the Rhodes Cyclonic area and the Ierapetra, the Shikmona and the Latakia Anticyclonic areas. Following the Mid Mediterranean Jet, branches of water are moving towards the Northern-Western part of Mersa Matruh to reach the Rhodes and Ierapetra gyres and to the East towards the Shikmona and Latakia gyres. Additionally, a branch of water moves towards the Egyptian coasts and affects also negatively the Chla concentrations of the area. The effect of the SSTA of Mersa Matruh Anticyclone is continuing also during May (Fig. 2), but with much less effect. In this month branches of water move towards the Southern Levantine basin and seem to affect negatively the Chla concentrations at the Egyptian coasts.

Regarding the indirect relations, SSTA in Mersa Matruh Anticyclone has been highly negatively correlated to ChlaA in the Southern Aegean as well as the Western Mediterranean basin during April. During May it appeared to be highly anticorrelated with Adriatic and Ionian Seas as well as the areas at the coasts of Libya and Algeria.

These results give an indication that Mersa Matruh can be an index of the SST and Chla situation in the Mediterranean Sea and as it is described in section 3.4.1 it could represent the teleconnections between larger scale phenomena.

Effects in Terrestrial Productivity

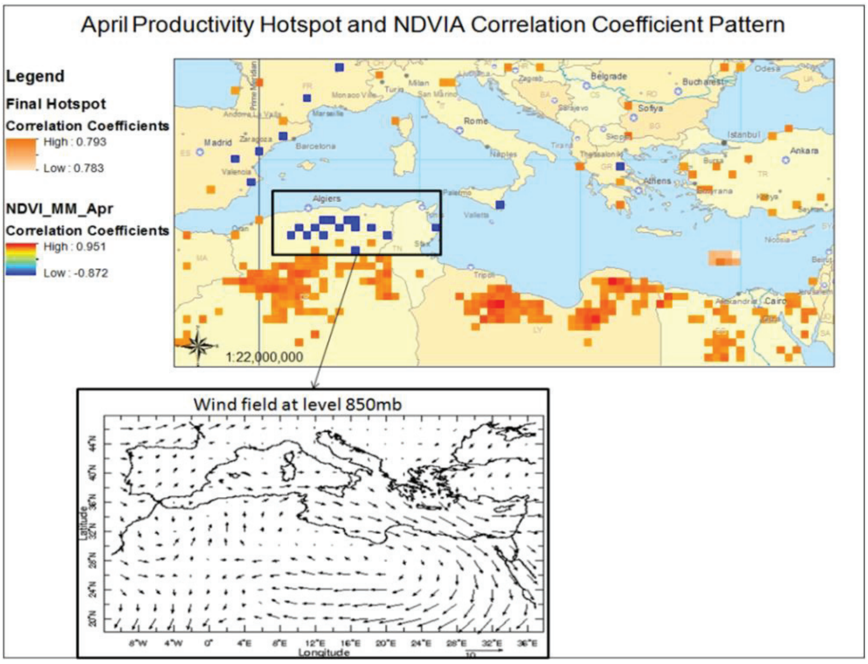

Fig. 3: Productivity Hotspot in April (Mersa Matruh Anticyclone) and the average NDVIA Correlation Coefficient pattern around the Mediterranean Sea (upper image). Highlighted are the wind velocity vectors of the area of interest.

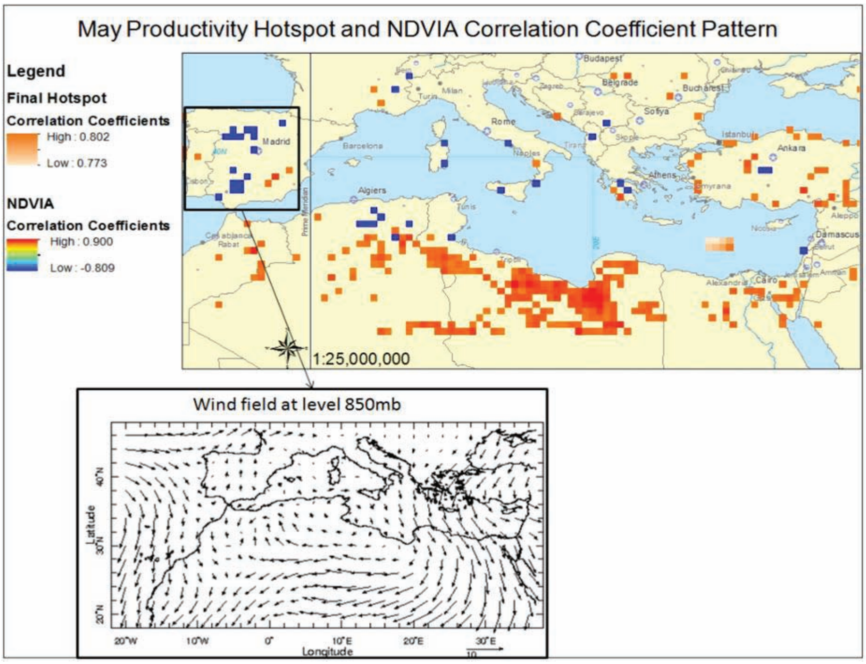

Fig. 4: Productivity Hotspot in May (Mersa Matruh Anticyclone) and the average NDVIA Correlation Coefficient pattern around the Mediterranean Sea (upper image). Highlighted are the wind velocity vectors of the area of interest.

The Libya atmospheric anticyclone seems to be the reason of the negative effects of Mersa Matruh gyre on vegetation in Algeria in April (Fig. 3) and Spain in May (Fig 4). Warm advection (Lolis, et al., 2002) and this anticyclone transfer the moisture further towards the Alps, where it causes abundant rainfalls (Baldi, et al., 2006). In agreement with that, the correlation process revealed positive correlation coefficients of SSTA in Mersa Matruh against RA in the Alps region during September, but it was also in not significant enough to be included in the effects of the studied gyre.The climate in the Central and South-eastern Spain is Mediterranean with the latter area presenting also semi-arid characteristics (Garcia- Gomez 2011). In agreement with the case of Algeria described previously, the moisturised air in this case is transferred in Northern and Central France where positive, but still not significant, correlations where identified